Histol Histopathol (1996) 11: 965-984

Histology and Histopathology

Description of primordial germ cells, oogonia, oocytes and embryo-like growth in squash preparations of tissues from hematological malignancies

H. Logothetou-Rella

Department of Experimental Physiology, Medical School, University of Athens, Athens, Greece

Summary. This study evidences the presence of primordial germ cells, in tissue squash preparations and sections from hematological malignancies. Primordial germ cells were identified by their morphology, the intense PAS, PAS-D reaction and presence of calcium-activated neutral proteinase. Primordial germ cells gave rise to nuclear vlimata. Immature oogonia exhibited a nuclear envelope and a star-shaped nuclear core, arising from acellular globose bodies impregnated by a nuclear vlima of primordial germ cell. Bone marrow tissue oogonia were PAS and PAS-D positive, identical to fungal ones. Calcium-activated neutral proteinase was demonstrated in the plasma of the acellular globose bodies, the nuclear envelope and the conglomerated primordial germ cells. Immature bone marrow oogonia progressed into mature ones, leptotene, diplotene, dictyotene and mature oocytes. Nuclear vlimata fertilized primordial germ cells, oogonia and oocytes, giving rise to round embryos at the morula and hatching morula-like stages. Embryos consisted of a zona-pellucida-like cortex, composed of glycosaminoglycans, glycoproteins, protease and diffuse nuclear material, enclosing developing cells. Primordial germ cells, oogonia and embryos were also demonstrated in squash preparations of adult rat testis and sections of normal rat bone marrow tissues. The observations document that primordial germ cells are the primary stem cells which give rise to nuclear vlimata and oogonia, which constitute the secondary stem germ cells. The results are discussed in terms of stem cell renewal according to the events: primordial germ cells - gametes - fertilization - embryos - primordial germ cells.

Key words: Primordial germ cells, Oogonia, Fertilization, Embryos, Malignancy, Fungi, Testis, Calcium-activated neutral proteinase

Offprint requests to: Dr. Helen Logothetou-Rella, Department of Experimental Physiology, Medical School, University of Athens, P.O. Box 60114, GR153-10 Agia Paraskevi, Athens, Greece

Introduction

It has recently been observed that malignant bone marrow cells (BMC) divide by abnormal meiosis, in vitro and in vivo, giving rise to male and female-like gametes. Nuclear vlimata (NVs), the male gametes were of head with tail morphology, carrying aneuploid sets of chromosomes (Logothetou-Rella, 1996).

Aneuploid or diploid oocyte-like metaphases were detected, similar to those of a mature human oocyte. NVs invaded host cells, decondensed and implanted their chromosomes into host cells in metaphase, with a process similar to fertilization. Fertilization was documented by metaphases exhibiting both the female and male meiotic sex chromosomes. NV invasion was achieved via the calcium-activated neutral proteinase (CANP), distributed in the NV head and meiotic chromosomes (Logothetou-Rella, 1996).

BMC communicated by nuclear bridges (NBs) through which whole chromosomes were transferred and exhibited the characteristic events of somatic cell meiosis, such as: nuclear extrusion of chromosomes, NVs formation, metaphase and nuclear fusion, hybrid metaphases, nuclear budding, nuclear conglomerates (NCs), NBs, chromosomal fusion substance (CFS), transfer of chromosomes and aneuploidy (Logothetou-Rella, 1995a, 1996).

In this study, the presence of primordial germ cells (PGC), oogonia (Ogs), oocytes and embryo like-growth is investigated in squash preparations from hematological malignancies using fungal and rat testicular cells as control cell systems.

Materials and methods

Cytogenetic, morphology, cytology and immunocyto-chemistry of PGCs, oogonia, oocytes and embryos

A total of thirteen cases of hematological malignancies were examined. One case of erythro-

leukemia (EL), four cases of acute myeloid leukemia (AML-1, AML-2), two cases of acute myelomonocytic leukemia (AMMol-M4) two cases of undifferentiated leukemia (UL-1, UL-2), one case of chronic myelogenous leukemia (CML) and three cases of acute lymphoblastic leukemia (ALL). Patients had received no treatment prior to aspirate collection. Small bone marrow tissue (BMT) pieces, washed in phosphate-buffered saline (PBS), were treated with KCl (0.075M) for 10 min, fixed in 3:1 ethanol:acetic acid for 24 hours, followed by 6:4 acetic acid:distilled water for 5 min, squashed on glass slides, dried and stained with Giemsa, PAS, PAS-D for cytogenetic morphology. Squashed BMT, after KCl treatment, fixed in 4% formaldehyde in PBS were stained with Feulgen (without counterstain), or immunostained for α_1-antichymotrypsin.

Isolated BMC from two cases of AML, growing attached on the culture vessel surface in the presence of phytohaemaglutinin (PHA) (Logothetou-Rella, 1996), were treated with KCl for 10 min (HT), fixed in 4% formaldehyde in PBS for PAS, PAS-D staining and immunocytochemistry. For immunocytochemical studies the avidin-biotin peroxidase complex method was applied (Hsu et al., 1981) using the antiserum against α_1-chymotrypsin (1:100, A022, Dako Corp.). Positive and negative controls were used.

Testis, of 1-8-week-old Wistar rats were removed, sliced, treated with KCl (0.075M) for 10 min squashed on slides and stained with Giemsa, PAS and PAS-D.

Three types of fungus, *Dermatophyte microsporum* sp., *Aspergillus fumigatus* and *Candida albicans* were used for cytogenetic morphology, PAS and PAS-D staining and immunocytochemistry as previously described (Logothetou-Rella, 1996). Ten serial BMT paraffin sections from 10 cases of CML, 10 cases of AML and 5 cases of MDS were stained with Giemsa, PAS, PAS-D, and immunostained using the antiserum against α_1-chymotrypsin (1:1000, A022, Dako Corp.), using negative and positive controls (Hsu et al., 1981).

Results

Cytogenetic, morphology, cytology and immunocytochemistry of primordial germ cells, oogonia, oocytes and embryos

All tissue squash preparations exhibited immature and mature exfoliated Ogs (Fig. 1). Various-sized acellular globose bodies (AGBs) (Fig. 1a), embraced by nuclear segments arising from crescentic conglomerated nuclei (Fig. 1b) or impregnated by a NV (Fig. 1c,d), or containing a nuclear star-shaped core with or without spokes (Fig. 1e,f), were the immature forms of Og. Mature Ogs were characterized by a complete, intact nucleus. Some mature Ogs contained a round, hyperchromatic, condensed nucleus (Fig. 1g), while others a larger one with dispersed chromatin (Fig. 1h,i). The various-sized Og contained various numbers of double minutes (DMs), minute and ring chromosomes, surrounded by a thin or thick nuclear envelope (NE) (Fig. 1j,k). Ogs of a full nucleus were surrounded and invaded by NVs (Fig. 1l,m). Og appeared single or in clusters encircled by nuclear segments arising from conglomerated crescentic nuclei (Fig. 1n,o). Large immature Og divided by budding to smaller daughter cells containing DMs (Fig. 2a). Og also arose within large NCs (Fig. 2b) which extended nuclear segments embracing and forming the NE of Og (Fig. 2c). Conglomerated nuclei free of Ogs were present (Fig. 2d).

Progression of Og to oocytes was documented by the presence of leptotene (Fig. 2e,f), diplotene (Fig. 2g) and dictyotene (Fig. 2h) stages of the first meiotic prophase. Dictyotene-stage oocytes were in various sizes within the same sample, been characterized by the lacy network of chromatin.

Oocytic metaphases were identified by chromosomes identical to those of a human mature oocyte (Fig. 2i) (Plachot et al., 1987). Most oocytes consisted of meiotic condensed prochromosomes (Fig. 2j-n). Some oocytes kept the NE consisting of DMs and minute chromosomes (Fig. 2k). Abnormal metaphases of fertilized oocyte (Plachot et al., 1987) were present, showing two female «0» chromosomes, one «Y», one bivalent «XY» and a marker chromosome in one metaphase from a male patient (Fig. 2o).

Presence and formation of Og was confirmed by PAS and PAS-D staining (Fig. 3). The plasma of the AGBs, immature and mature Ogs, were PAS and PAS-D positive, consisting of glycogen, glycoproteins and glycosaminoglycans (GAG). Ogs were in clusters, embraced by thick nuclear segments, implanted in the tissue, or exfoliated. Upon exfoliation large round unstained vacuoles remained on tissues, surrounded by

Fig. 1. AGB, immature and mature Og. **Inset a:** various-sized exfoliated AGB. **Inset b:** crescentic, conglomerated nucleus extends nuclear segments embracing the AGB, forming a NE. **Insets c and d:** AGB impregnated by a NV. **Insets e and f:** immature Og with star-shaped nuclear core and NE. **Inset g:** mature Og with a small, round, condensed nucleus. **Insets h and i:** mature Og with large, round nucleus with dispersed chromatin. **Insets j and k:** immature Og with DMs, ring and minute chromosomes. **Inset l:** figure focused on NV embracing Og. **Inset m:** mature Og fertilized by two NVs. **Insets n and o:** Ogs in clusters, held together by nuclear segments arisen from conglomerated, crescentic cells. Giemsa. x 1,000

Fig. 2. Female gametes in BMT squash preparations. **Inset a;** dividing Og by budding. Daughter Og (arrow) contains a DM. **Inset b:** conglomerated nucleus bearing an Og. Giemsa. x 1,000. **Inset c:** nuclear conglomerate extends thick nuclear segments embracing Ogs. Giemsa. x 400. **Inset d:** conglomerated nucleus free of Og. Giemsa x 1,000. **Inset e and f:** leptotene-stage oocytes. **Inset g:** diplotene-stage oocyte. Giemsa. x 1,000. **Inset h:** dictyotene-stage oocytes of various size and lacy network of chromatin. Giemsa. x 100. **Inset i:** metaphase with chromosomes of a mature human oocyte. **Insets j-n:** oocytes with meiotic, condensed prochromosomes with or without a NE. Giemsa. x 1,000. **Inset o:** a metaphase of a fertilized oocyte showing two female chromosomes «0», one «Y», one bivalent «XY» and a marker chromosome. Giemsa. x 1,000

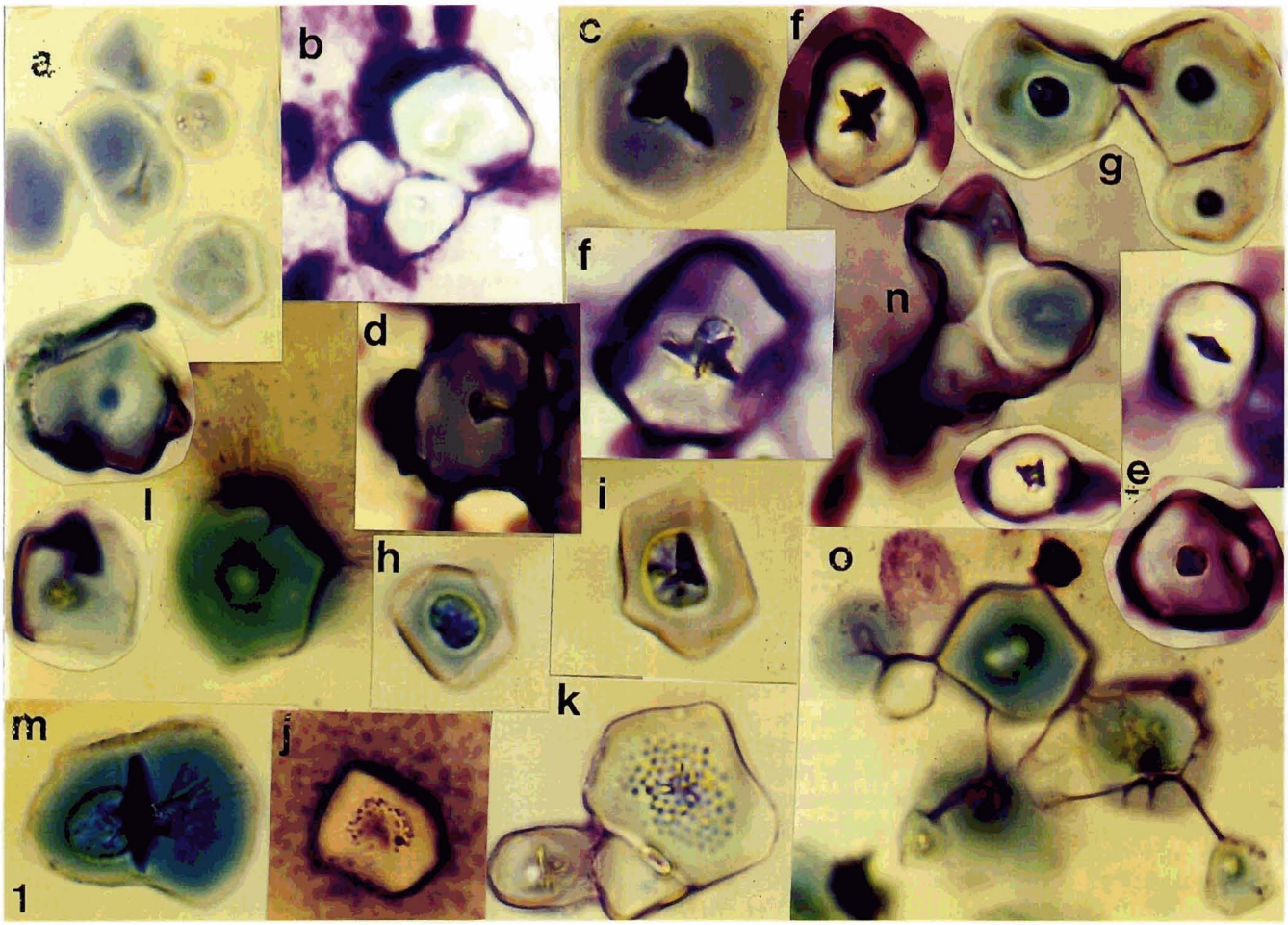
a
b
c
f
g
f
n
d
e
l
i
h
o
k
m
j
1

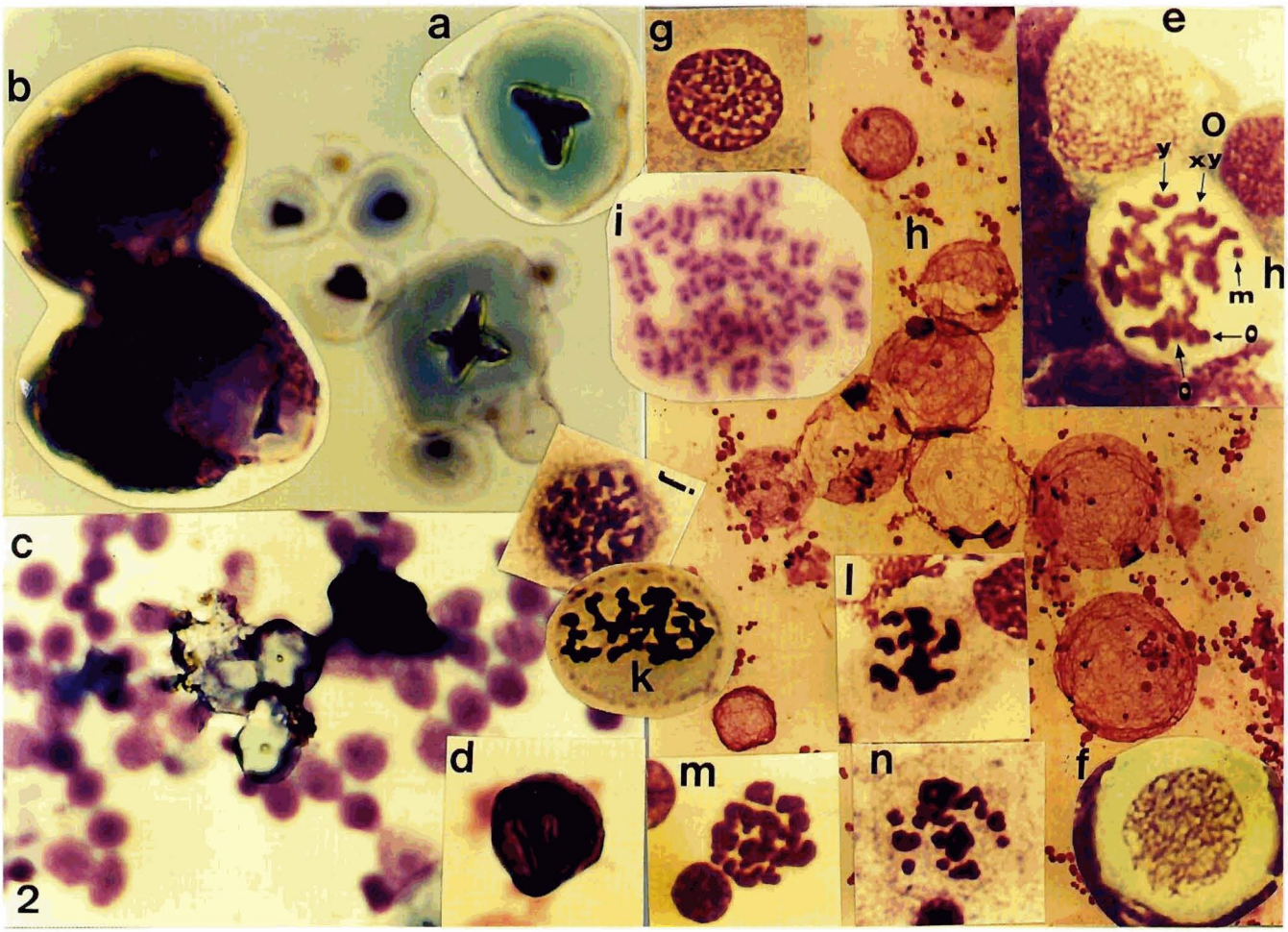
a
b
g
e
O
y
xy
i
h
h
m
o
o
l
k
c
d
m
n
f
2

thick nuclear segments (Fig. 3c). It was obvious that no fungal cells were associated with the Ogs. Conglomerated nuclei gave rise to nuclear segments embracing the AGB and/or nuclear spokes or NVs which impregnated the AGB forming the nuclear core of the immature Og (Fig. 4). Some AGB showed stained and unstained PAS-D areas (Fig. 4, 4a). Mature Og of complete, intact, large or small round nucleus were observed (Fig. 4b). The various possible morphologies of AGB, immature and mature Og were shown in Fig. 5. AGB impregnated by a NV (Fig. 5a) or immature Og embraced (Fig. 5b) or impregnated by a NV (Fig. 5c) were obvious. The content of AGBs showed PAS-D negative or mixed negative with positive or positive areas (Fig. 5d-f).

Og formation was also apparent in Feulgen stained preparations. Unstained AGB (Fig. 6, 6a) were impregnated by Feulgen-positive nuclear spokes or NVs arising from the NE, transfering DNA to the center of the AGB (Fig. 6b). Feulgen stained the NE, the core of Ogs (Fig. 6, 6b) and the nuclear rings and segments, red with dark blue or dark blue in spite of the omission of counterstain (Fig. 6c). Regular chromosomes were stained red (Fig. 6d) and pachytene ones red with dark blue chromomeres (Fig. 6e).

In squash PAS-stained preparations, PGCs were identified by: the two prominent nucleoli (Fig. 7a), round, large nucleus (Fig. 7b-d), the amoeboid movement (Fig. 7a, e-g), the oval (Fig. 7b) or elliptical morphology (Fig. 7h) and mainly by the dark PAS stain reaction. A PGC of large, round nucleus, was surrounded and invaded by a NV (Fig. 7i-k). The NVs arose from surrounding crescentic, conglomerated nucleus. PGC were intensively PAS-D positive, some showing irregular conglomerated nucleus, indistinct from the cytoplasm (Fig. 7l), often with a NE, keeping a darker red colour than the Og. PGC embryos were large globose, PAS-D positive, of 2-3 nuclei (Fig. 7m-o) surrounded by a NE.

PAS-D-stained BMT smears showed conglomerated PGCs surrounding an Og (Fig. 8a), a NV embracing an immature Og (Fig. 8b), PAS-D negative AGB with positive NE (Fig. 8c), clusters of various-sized Ogs (Fig. 8d), various intensity of PAS-D reaction, nuclear size and morphology (Fig. 8d-i).

AGB, all forms of immature and mature Ogs and PGCs were identified in PAS-, PAS-D-stained paraffin tissue sections, from ALL, CML, MDS and AML (Fig. 9). Amoeboid shape (Fig. 9a) and conglomerated PGCs (Fig. 9b-e) with prominent nucleoli (Fig. 9d) associated closely with AGB and Og were observed, identical to those in squash preparations. AGB embraced by NV (Fig. 9f), NE of immature Og (Fig. 9g), Og with a star-shaped nuclear core (Fig. 9h) or NV (Fig. 9i) and mature Og (Fig. 9j) were apparent, all surrounded by crescentic or round BMC. The easy exfoliation of PGC and Og from tissues left behind large vacuoles with the surrounding cells.

The function of BMT oocytes and their fertilization by NVs was evidenced by the presence of embryo-like growth in squash preparations. Embryos were round and of various size and cell composition (Fig. 10), consisting of a zona-pellucida-like cortex enclosing NCs in

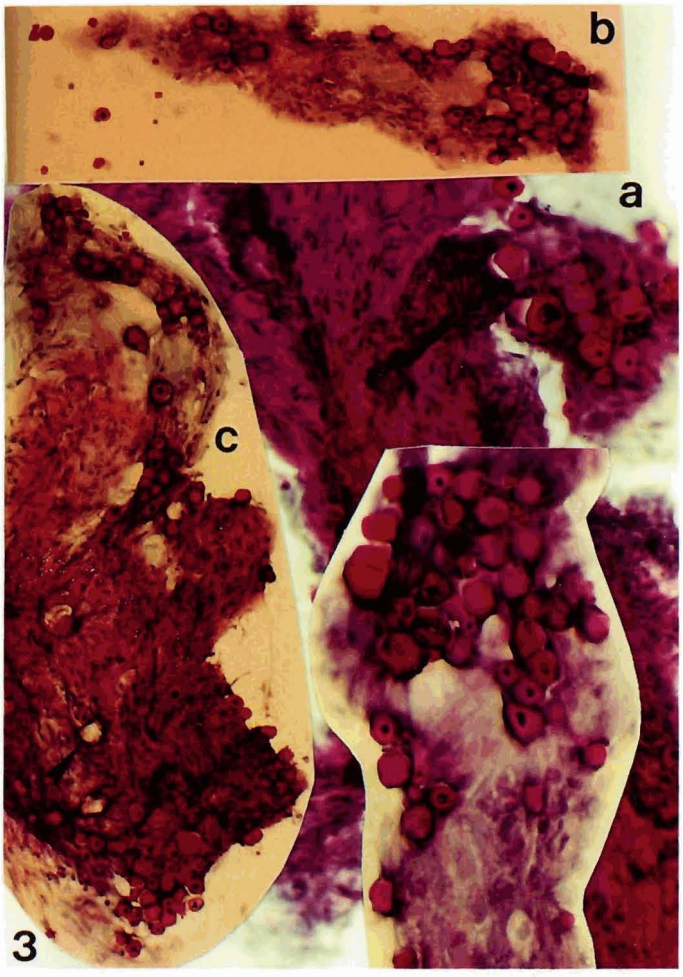

Fig. 3. GAG content of BMT Ogs. **Inset a:** AGB, immature and mature Og, embraced by nuclear segments, implanted in the tissue. PAS. x 200. **Insets b and c:** exfoliated Og leave empty round vacuoles (arrow) surrounded by nuclear segments. PAS-D. x 100

Fig. 4. AGBs with PAS-D stained and unstained areas, impregnated (arrows) by nuclear segments or NVs arisen from the surrounding cells or the nuclear envelope. PAS-D. x 1,000. **Inset a:** PAS-D negative AGBs. PAS-D. x 100. **Inset b:** mature Og of small or large round nucleus and clear, bright red cytoplasm. PAS. X 1,000

Fig. 5. Various morphologies of AGB, and Ogs. AGB with negative or negative and positive or positive PAS-D areas. **Inset a:** AGB impregnated by a NV. **Inset b:** an immature Og embraced by a NV. **Inset c:** an immature Og impregnated by a NV. **Insets d and e:** AGB with stained and unstained areas. **Inset f:** two AGBs one stained the other unstained. PAS-D. x 1,000

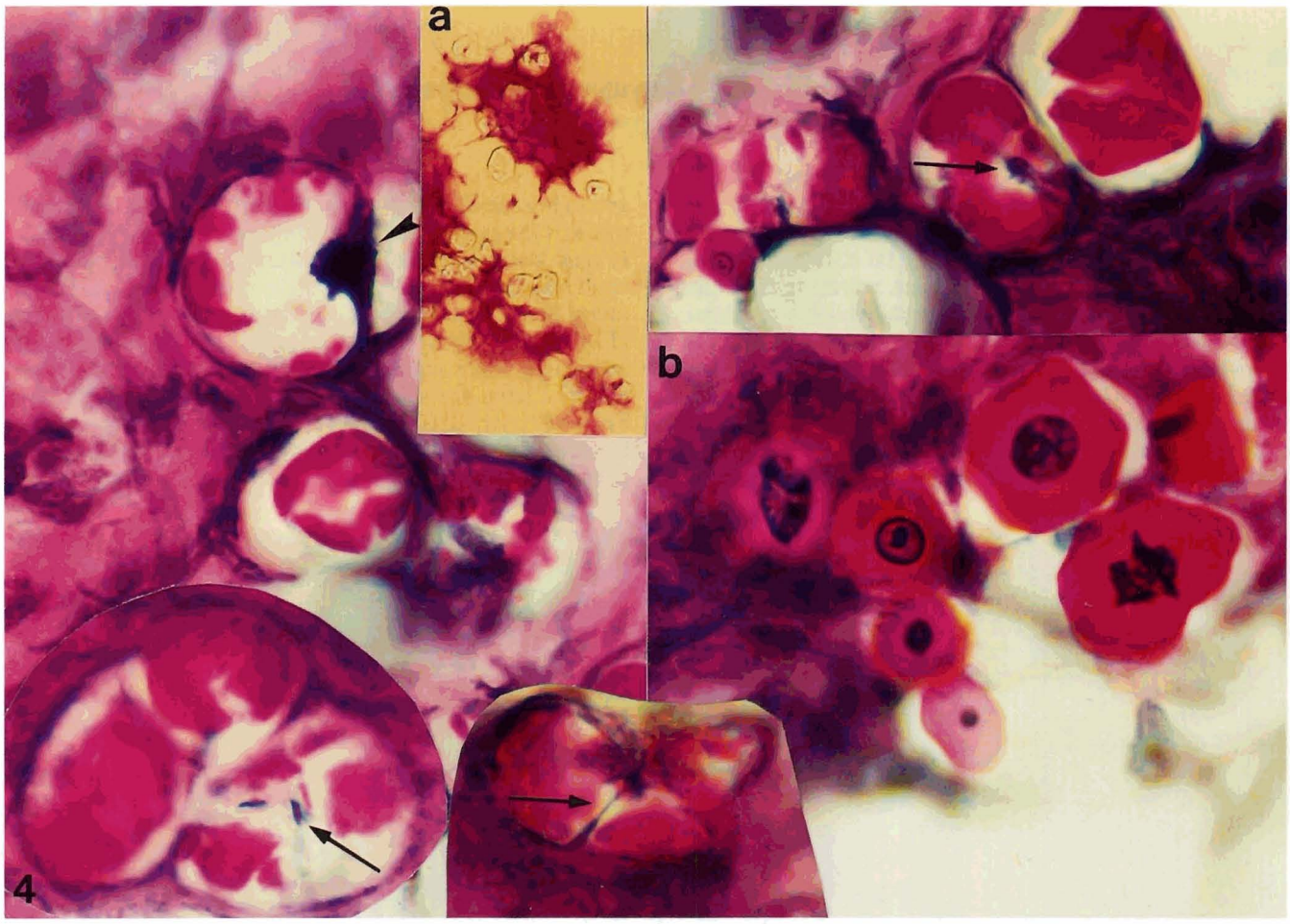
a
b
4

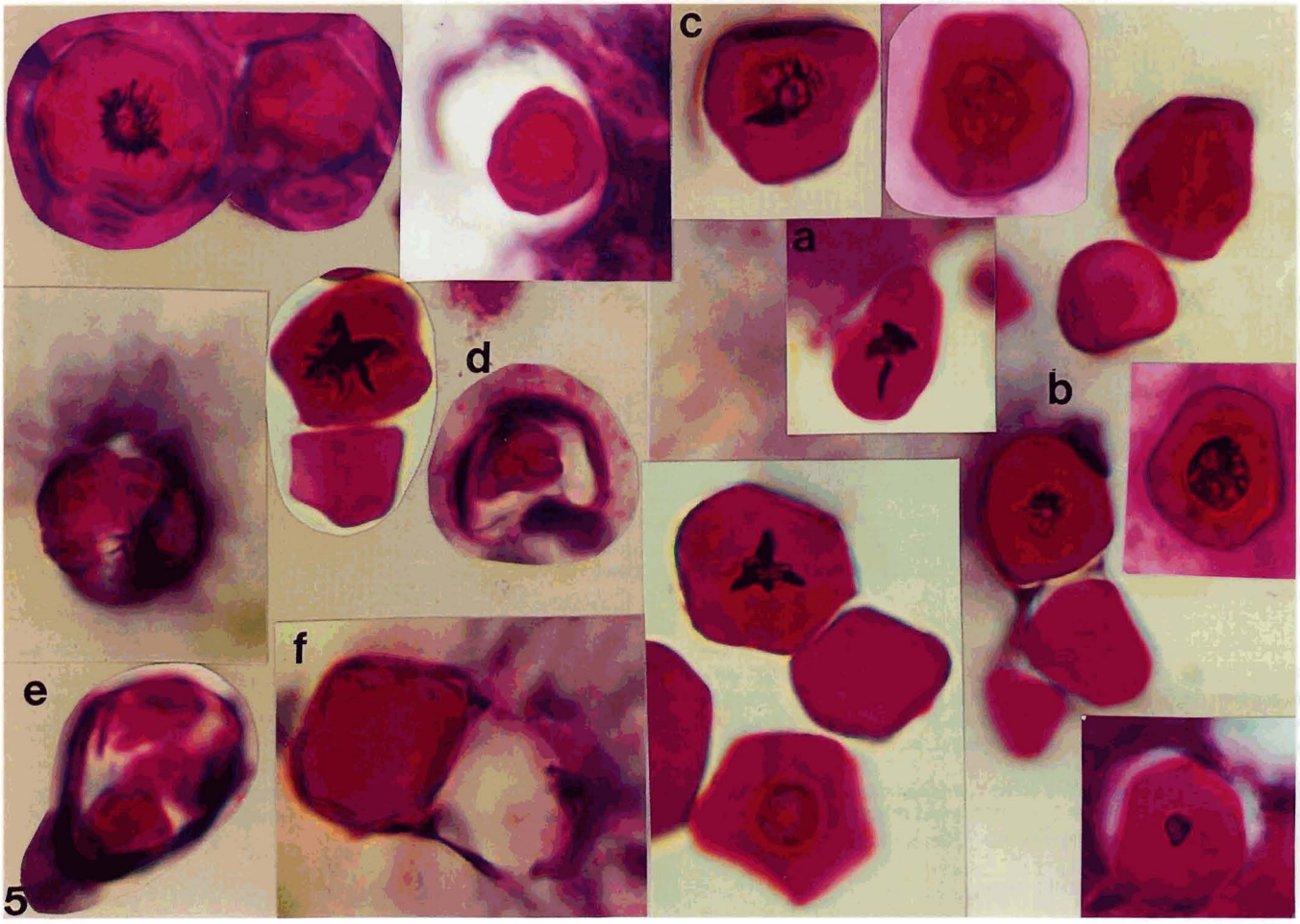
c
a
d
b
f
e
5

dissoluted nuclear material (Fig. 10a), or NCs, NVs and intact cells (Fig. 10b-f). Some embryos resembled uteral embryos at the morula stage (Fig. 10 c,d) and others resembled hatching morula (Fig. 10e), releasing the cells extraembryonically. Some embryos showed intact nuclei in the cortex (Fig. 10f). The cortex kept the cells enclosed even after tissue hypotonic treatment and squashing. Within the cortex of early embryos, dissoluted nuclear material, with or without circular nuclear segments (Fig. 11a,b), was condensing and organising itself into nuclei, which led to new nucleus and cell genesis (Fig. 11c,d). Formed cells were released towards the center of the developing embryos (Fig. 11e). It was clear that diffuse nuclear material gradually condensed giving rise to hyperchromatic intact nuclei, in towards the center and away from the embryo cortex (Fig. 12a). This observation was not considered artifactual since there was a continuance of the nuclear material from the cortex to the intact nuclei which co-existed with diffuse nuclear material (Fig. 12a). Developing cells within embryos exhibited the meiotic properties previously described (Logothetou-Rella,

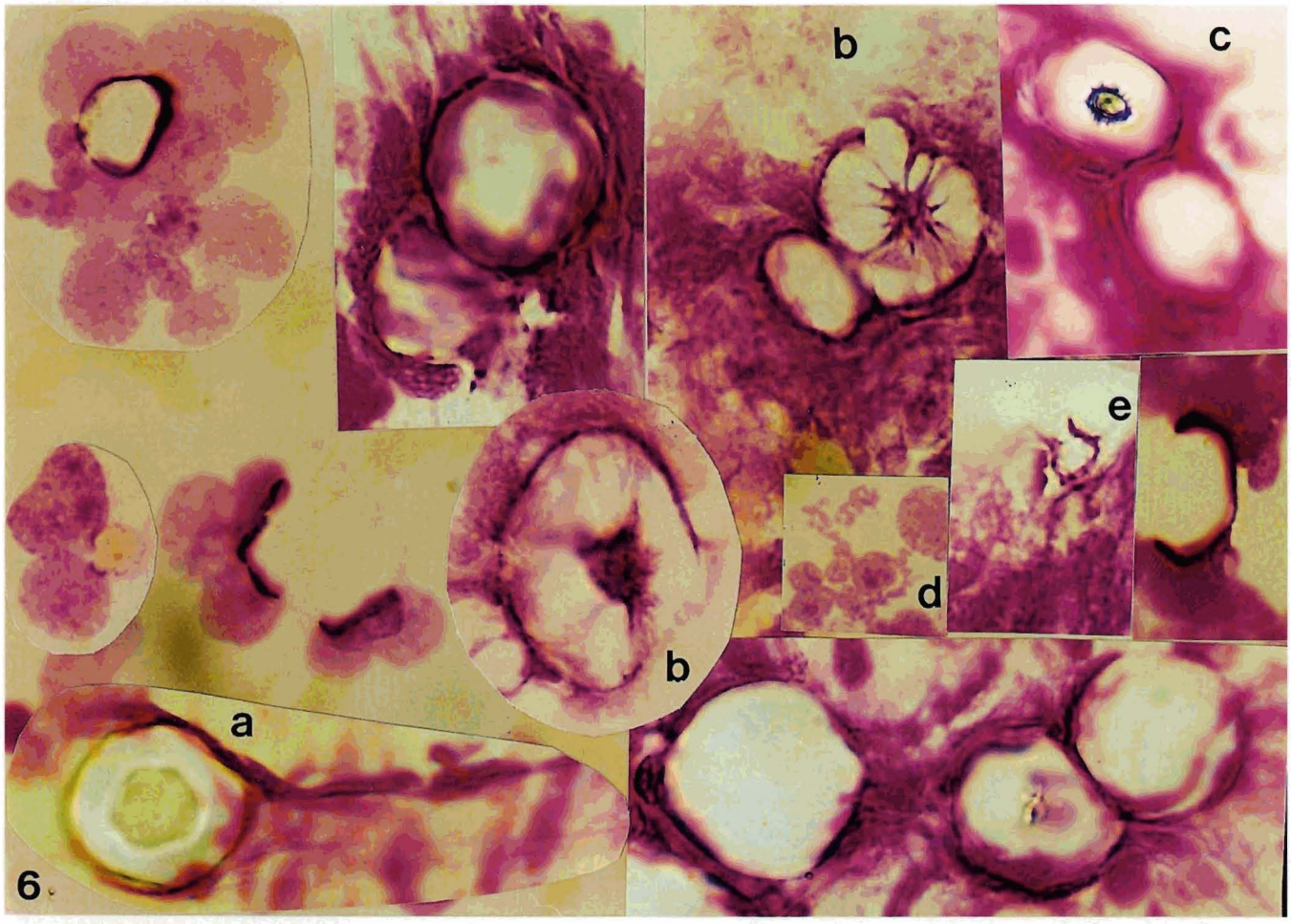

Fig. 6. Feulgen-stained nuclear rings, segments, NE and Og nuclear core red with dark blue or blue colour. **Inset a:** AGB free of DNA, surrounded by nuclear segments. **Inset b:** NV and/or spokes transverse and carry DNA from the NE to the center of AGB. **Inset c:** Og with nuclear core of blue colour. **Inset d:** regular chromosomes of red colour. **Inset e:** pachytene chromosomes with dark blue chromomeres. Feulgen (without counterstain). x 1,000

Fig. 7. Various morphologies of PGCs. **Inset a:** migrating PGC with two small prominent nucleoli. **Insets b-d:** oval-shaped PGC of large nucleus. **Insets e-g:** migrating PGC of NV morphology. **Inset h:** PGC of elliptical shape. PAS. x 1,000. **Inset i:** A PGC embraced by a NV. **Insets j and k:** PGC with NE, fertilized by a NV. **Inset l:** three conglomerated PGCs of irregular, diffuse nucleus, indistinct from the cytoplasm. **Inset m-o:** PGC globose embryos of two-three nuclei and NE. PAS-D. x 1,000

Fig. 8. PAS-D reaction of BMT smears. **Inset a:** conglomerated PGC surrounding an immature Og. **Inset b:** A NV embracing an Og. **Inset c:** negative AGB with positive NE. PAS-D. x 1,000. **Inset d:** Cluster of Ogs. PAS-D. x 400. **Insets e-h:** clusters of various-sized Ogs, various intensity of PAS-D reaction, nuclear size and morphology. PAS-D. x 1,000

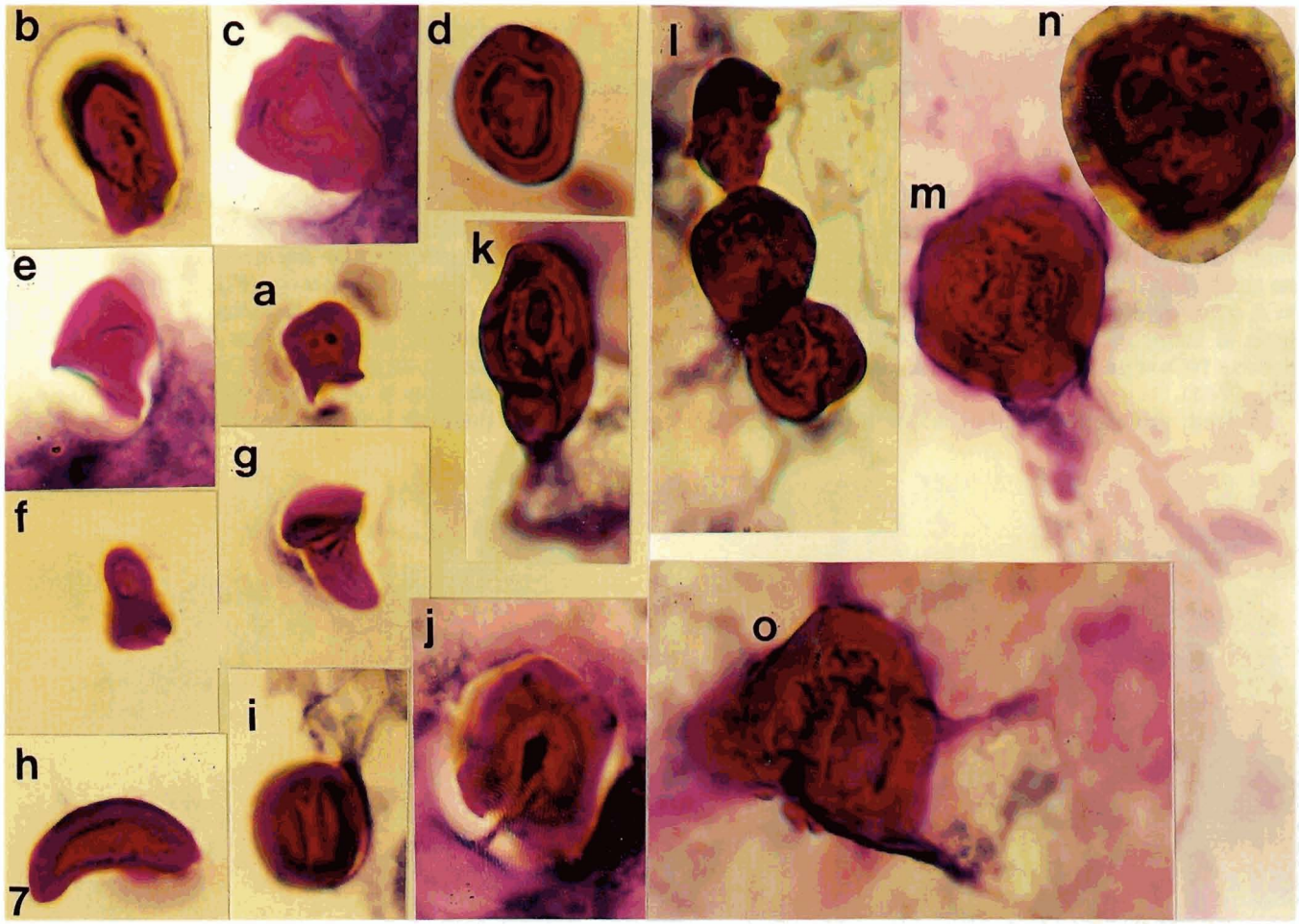
b
c
d
l
n
m
e
a
k
g
f
j
o
i
h
7

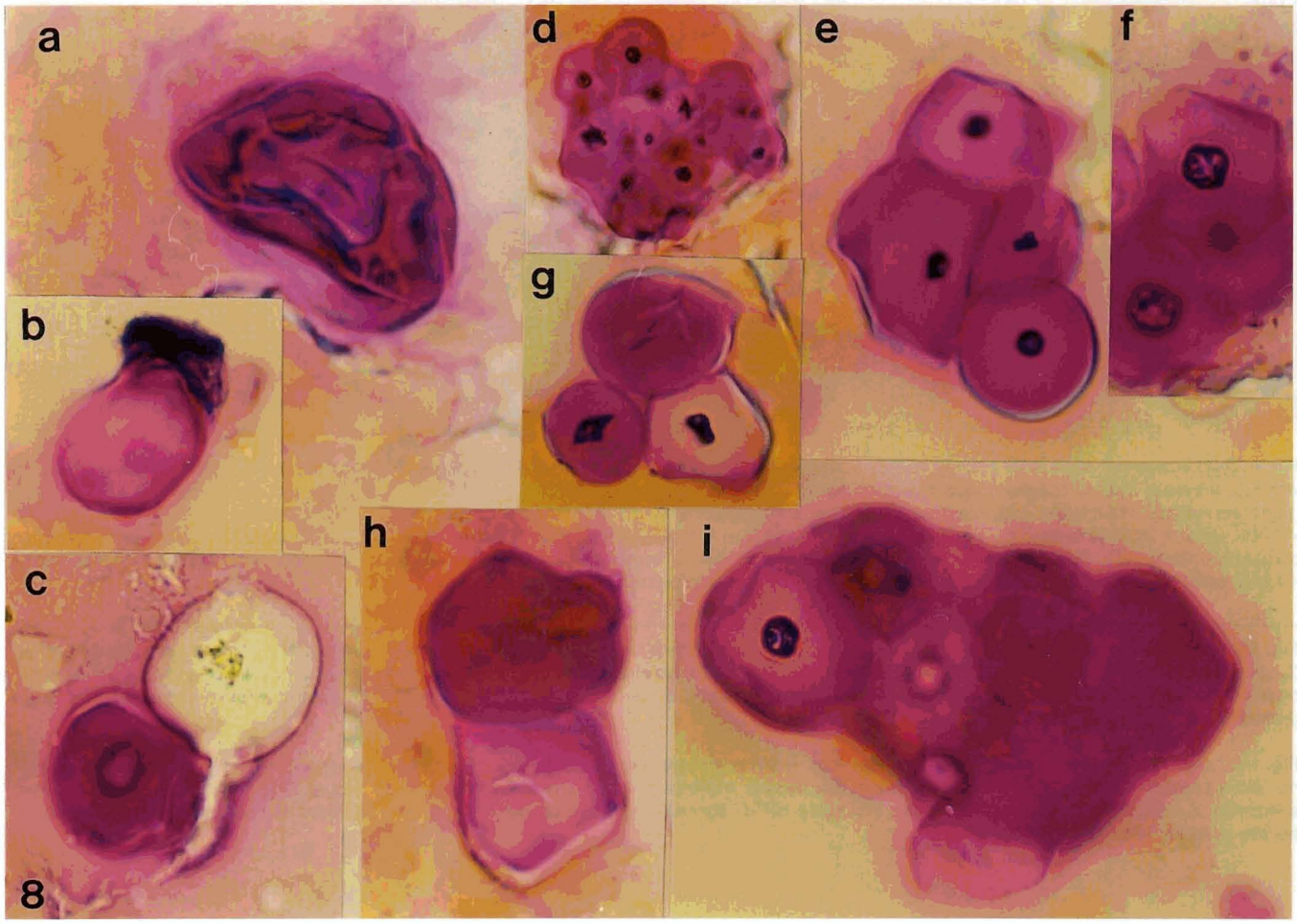
a
d
e
f
b
g
h
i
c
8

1996).

In cultured AML cells, fertilized Og (Fig. 12b), and small round embryos, with minute chromosomes inside the thick (Fig. 12c) or thin cortex (Fig. 12d) containing NCs, were evident. These embryos correlated well with those in histological sections from AML, consisting of globose NCs with a distinct cortex, embraced by a NV (Fig. 12e,f).

Within developing embryos, various-sized AGB (Fig. 13a), impregnated by NV and surrounded by scattered chromosomes were frequent (Fig. 13b,c). Intranuclear or extracellular nuclear rings, hyphae (Fig. 13d-f) and NCs giving rise to Og (Fig. 13g) or scattered chromosomes (Fig. 13h) were obvious.

The cortex of embryos was PAS and PAS-D positive, consisting of glycoproteins and GAG (Fig. 14). Also, round embryos in cultured AML cells showed PAS and PAS-D positive newly forming nuclei (Fig. 14a),

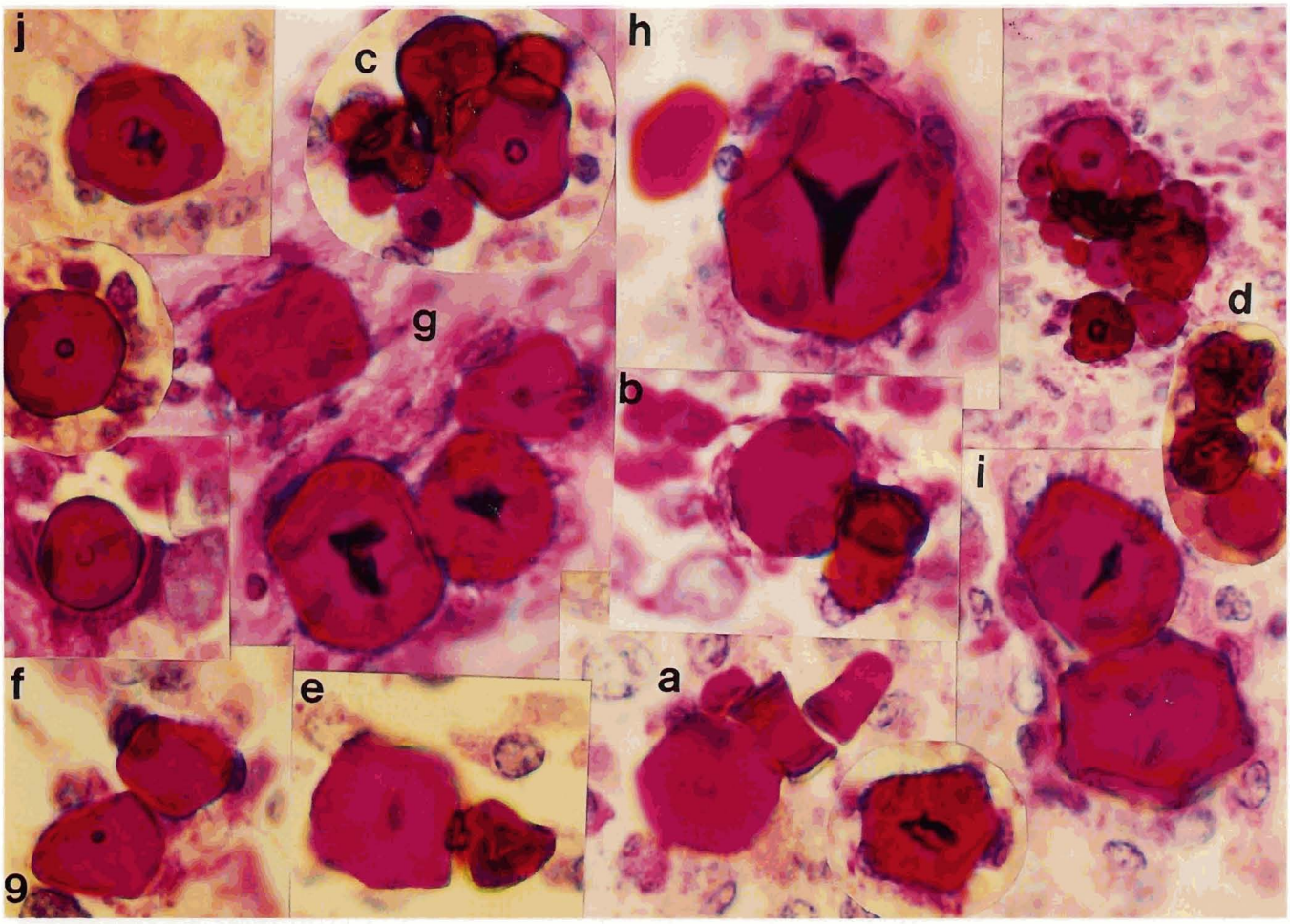

Fig. 9. GAG content of PGC, AGB and Og in AML tissue sections. **Inset a:** irregular morphology of migrating PGC of darker colour closely associated with Og. **Insets b and c:** conglomerated PGCs of darker colour, closely associated with Ogs. PAS. x 1,000. **Inset d:** conglomerated PGC or with prominent nucleoli and cluster of various-sized Ogs. PAS. x 400. **Inset e:** single conglomerated PGC associated with one Og (focus on PGC). PAS-D. x 1,000. **Inset f:** AGB embraced by a NV. **Inset g:** AGBs and Ogs with NE, implanted in the tissue (focus on NE). **Inset h:** a huge Og embraced by crescentic cells. **Inset i:** One AGB and one Og side by side surrounded by round epithelial cells. The Og shows a nuclear core of NV morphology. PAS. x 1,000. **Inset j:** a mature Og with large round nucleus similar to those in squash preparations. PAS-D. x 1,000

Fig. 10. Various-sized embryos showing a zona-pellucida-like cortex. **Inset a:** an embryo of a central NC surrounded by dissoluted nuclear material Giemsa. x 100. **Inset b:** embryo with NC, NVs and cells. Giemsa. x 400. **Inset c:** Giemsa. x 200. **Inset d:** embryo cortex contains faint nuclei (focus on cortex). Giemsa x 200. **Inset e:** hatching morula-like embryo, releasing cell extraembryonically. Giemsa. x 40. **Inset f:** embryo cortex contains cells. Giemsa. x 40

Fig. 11. Early embryos showing nucleus and cell genesis. **Inset a:** embryo shows circular nuclear segments in dissoluted nuclear material. There are no nuclei present. Giemsa. x 100. **Inset b:** dissoluted nuclear material in embryo reaching slight round shape (arrow). **Inset c:** embryo shows completed round-shaped nuclei with boundaries, inside the cortex. Surrounding nuclei are intact. Giemsa. x 200.**Inset d:** nucleus formed by dissoluted nuclear material. Giemsa. x 1,000

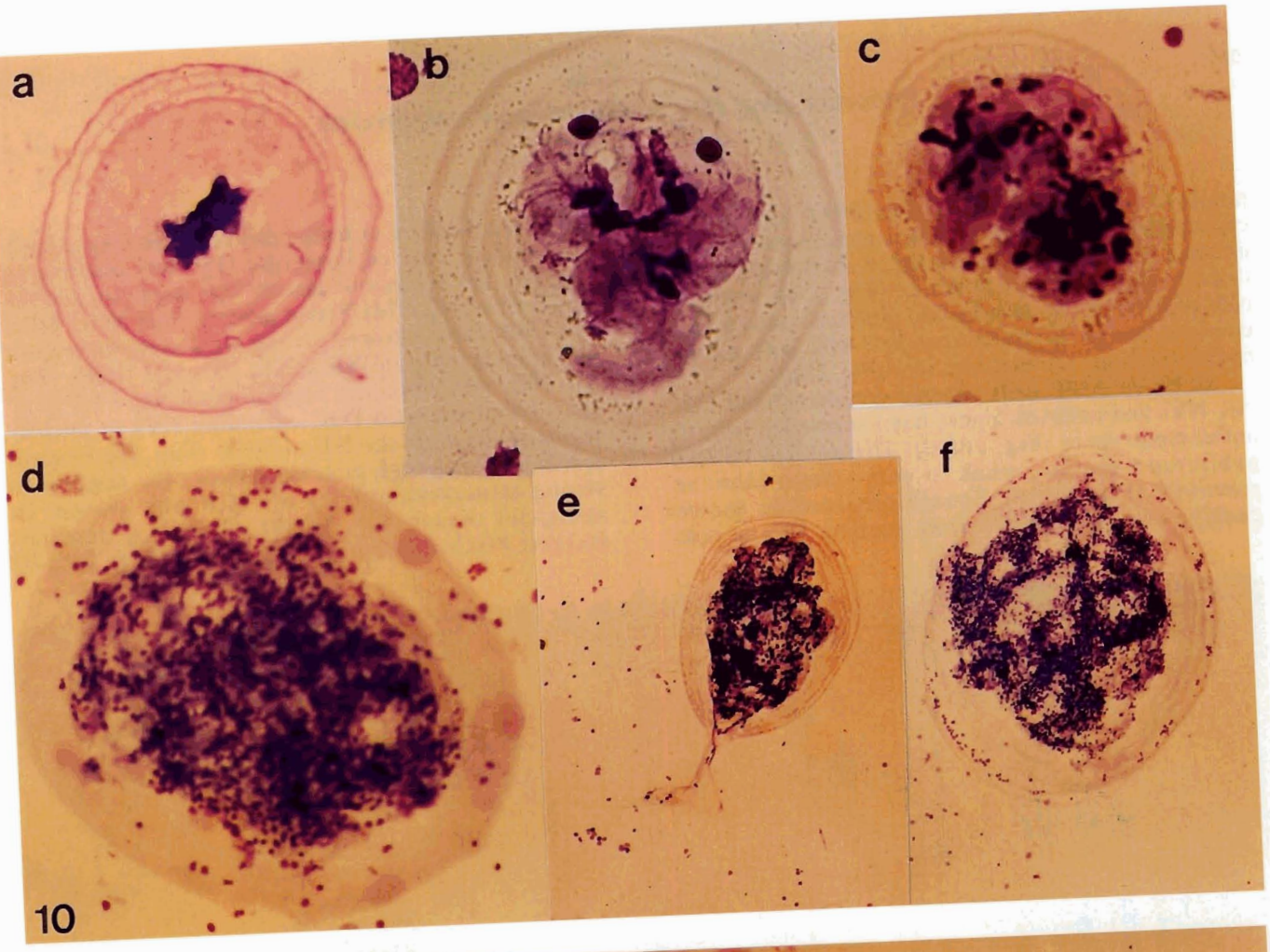

10

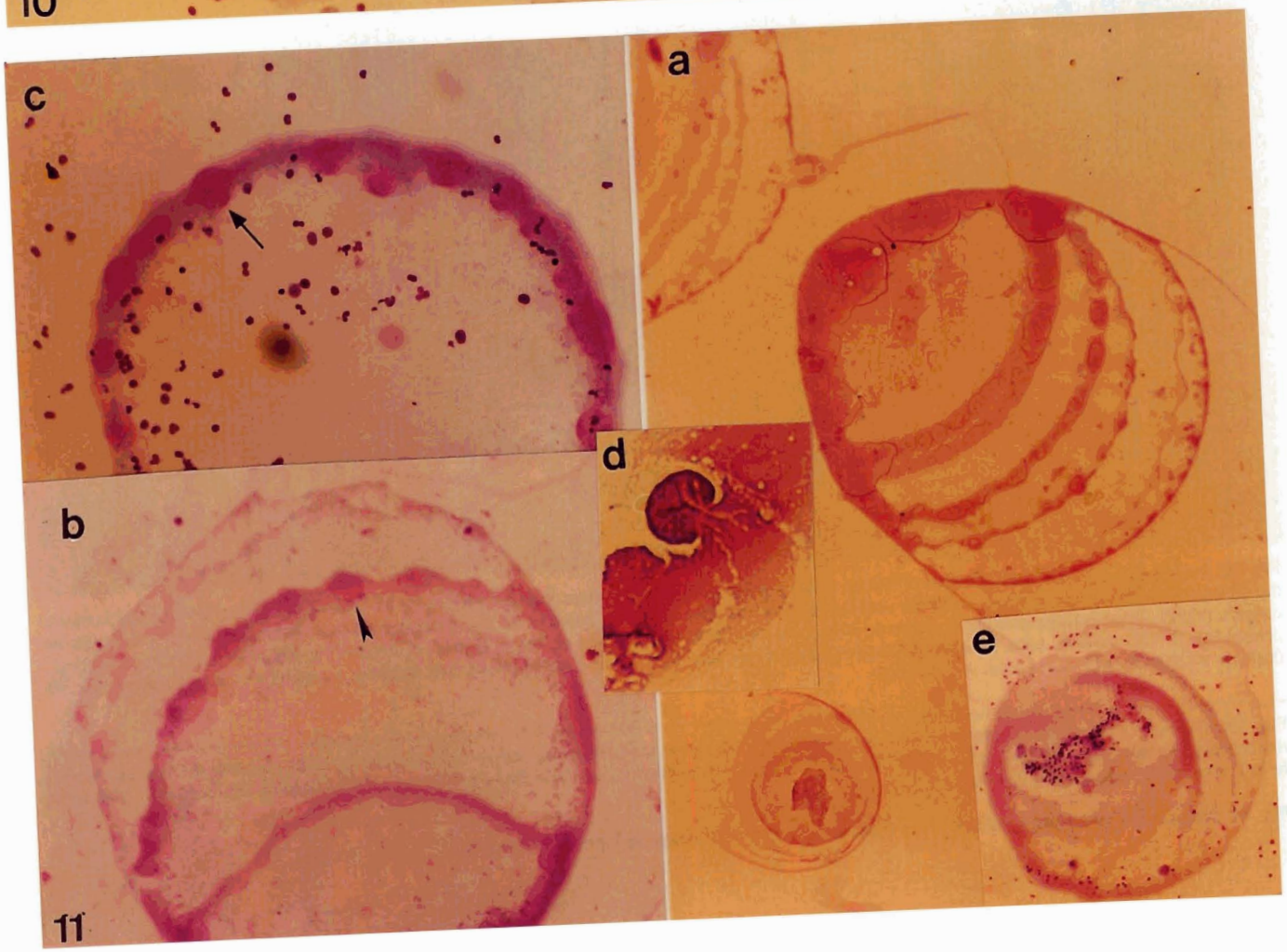

11

positive cortex with positive DMs and minute chromosomes (Fig. 15). Identical round embryos were demonstrated in AML histological section showing a discrete PAS and PAS-D cortex (Fig. 15a), enclosing cells of indistinct boundaries and prominent nuclei; these embryos morphologically correlate well with a 2-cell embryo in rat uteral tissue sections (Fig. 15b).

Cultured AML cells showed conglomerated PGC, NE, NVs and embryos highly immunoreactive with α_1-antichymotrypsin (Fig. 16a-d). The content of AGB exhibited negative, weak to very strong immunoreactivity (Fig. 16b-d). Squash preparations showed positive nuclear segments from positive NCs or cells, embracing negative to weak positive AGBs (Fig. 17a-c). The nuclear core of immature Ogs was positive to negative, the nucleus of mature Ogs negative, and the NE positive (Fig. 17d). Tissue sections from AML, MDS and CML, also showed strong α_1-antichymotrypsin immunoreactivity in PGCs, NE, NCs and AGBs (Fig. 18). PGC with prominent nucleoli producing a NV (Fig. 18a), conglomerated PGC extending NVs or nuclear segments forming the NE of AGB (Fig. 18b-e) were events involving high protease activity. The negative to strong immunoreactivity of AGB was evident in malignant tissues (Fig. 18b-e). Migrating, immunostained PGC of prominent nucleoli (Fig. 18f) or

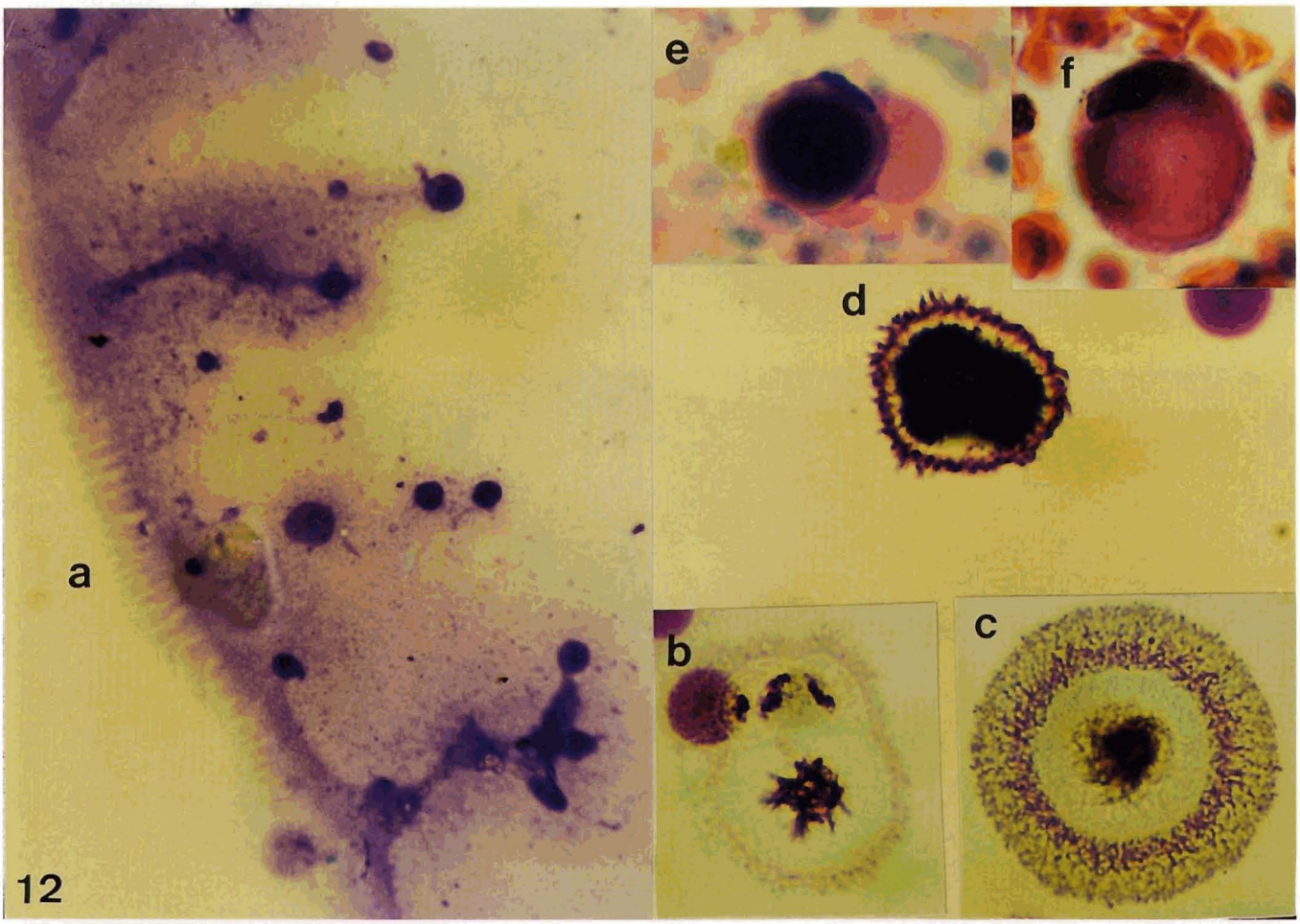

Fig. 12. Inset a: progressive condensation of diffuse nuclear material leads to nucleus genesis starting from the embryo cortex, towards the center of the embryo. Diffuse nuclear material co-exists with intact nuclei. Giemsa. x 1,000. **Inset b:** an Og fertilized by a four-chromosome NV. The Og shows conglomerated chromosomes and NE, in cultured AML cells. **Insets c and d:** early embryos of thick or thin cortex with chromosomes containing a central NC, in cultured AML cells. **inset e:** globose conglomerated embryo in MDS histological picture, showing a distinct cortex, embraced by a NV. Giemsa. x 1,000. **Inset f:** same as e. H-E. x 1,000

Fig. 13. Content of embryos. **Insets a-c:** AGB surrounded by scattered chromosomes and/or impregnated by a NV. **Insets d-f:** intranuclear or extracellular nuclear rings, hyphae and nuclei in dissoluted nuclear matrix. Giemsa. x 1,000. **Inset g:** embryo with NC bearing Og. Giemsa. x 200. **Inset h:** NC releasing chromosomes. Giemsa. x 1,000

Fig. 14. GAG content of embryos. PAS-D. x 40. **Inset a:** cultured AML embryo with newly forming nuclei. PAS-D. x 1,000

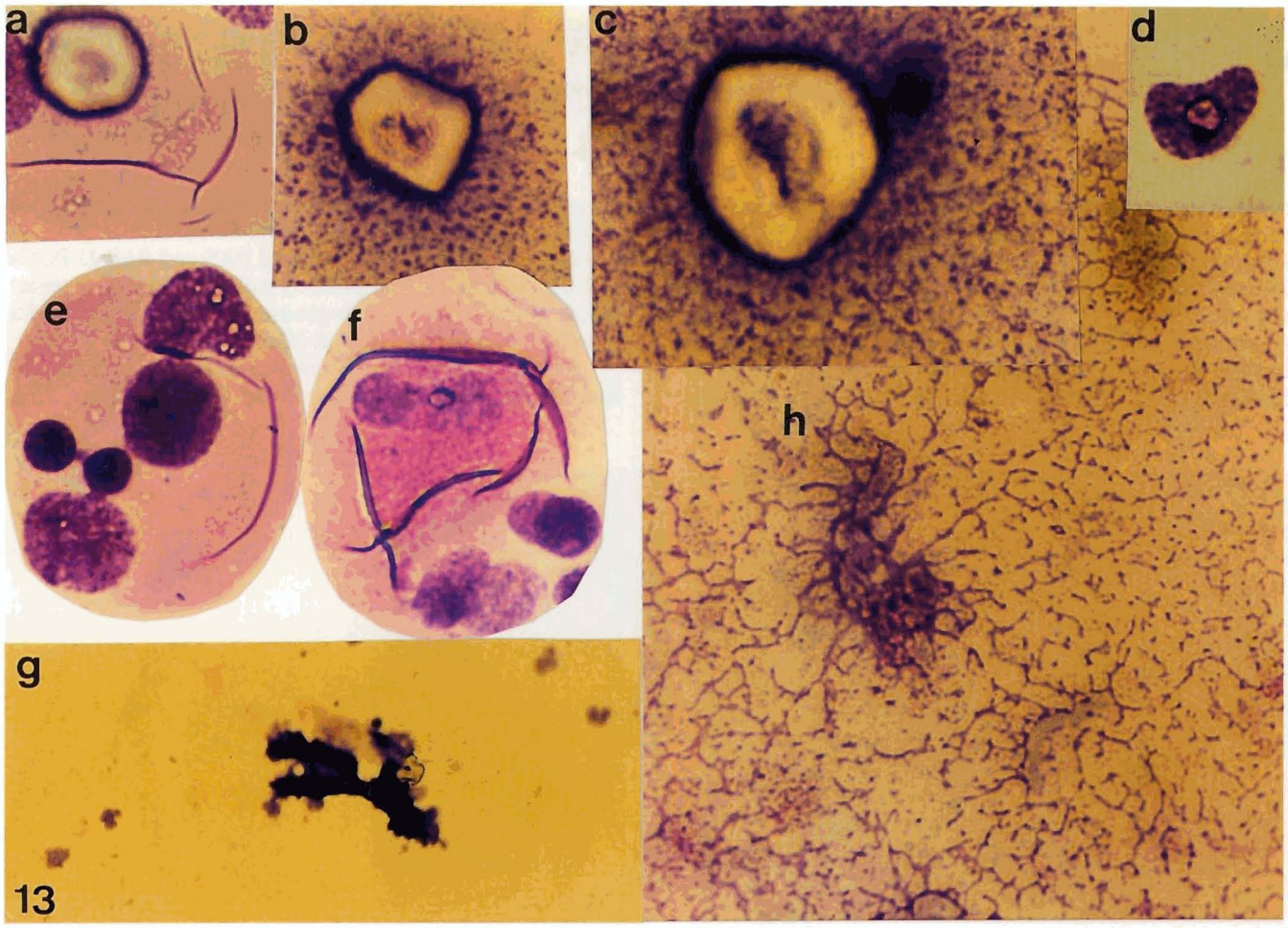
a
b
c
d
e
f
g
h
13

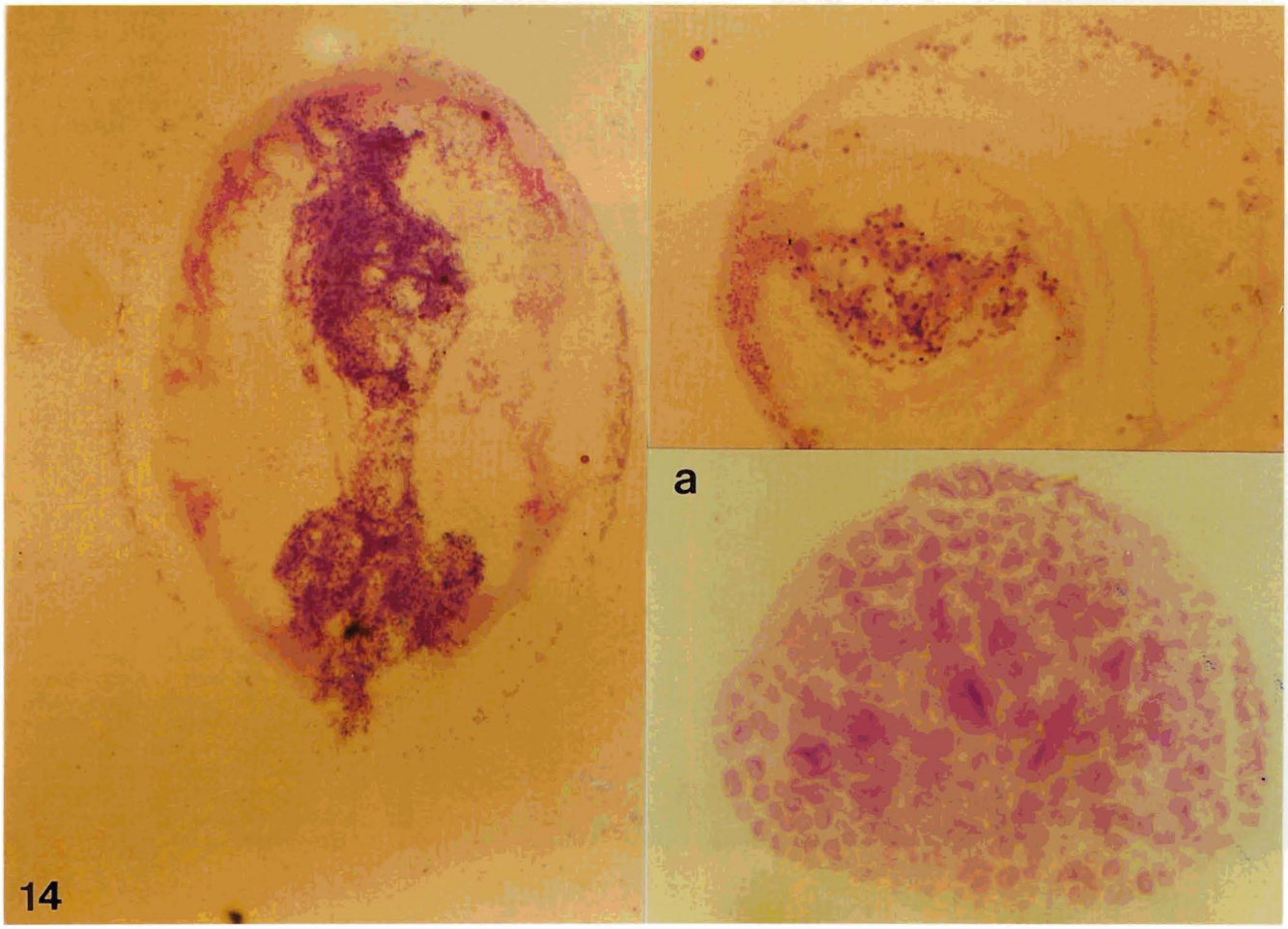
a
14

conglomerated nucleus (Fig. 18g) of NV morphology, oocyte-like cells with immunostained NE and NCs (Fig. 18h), globose embryos with immunostained NE (Fig. 18i) and/or cells (Fig. 18j) were obvious. Mature Og showed negative plasma but positive NE and surrounding cells (Fig. 18k). Megakaryocytes were devoid of a NE and α_1-antichymotrypsin immunoreactivity (Fig. 18l), distinguishing them from embryos. Assembly of immunoreactive chromosomes around an AGB could be seen in tissues (Fig. 18m).

Normal rat BMT also showed PAS and PAS-D PGCs and Ogs which were implanted and surrounded by tissue matrix only (Fig. 19). Cytogenetic morphology showed a few hollow embryos, devoid of cells.

The cytogenetic morphology and formation of fungal Og was identical to those of BMT (Fig. 20a).

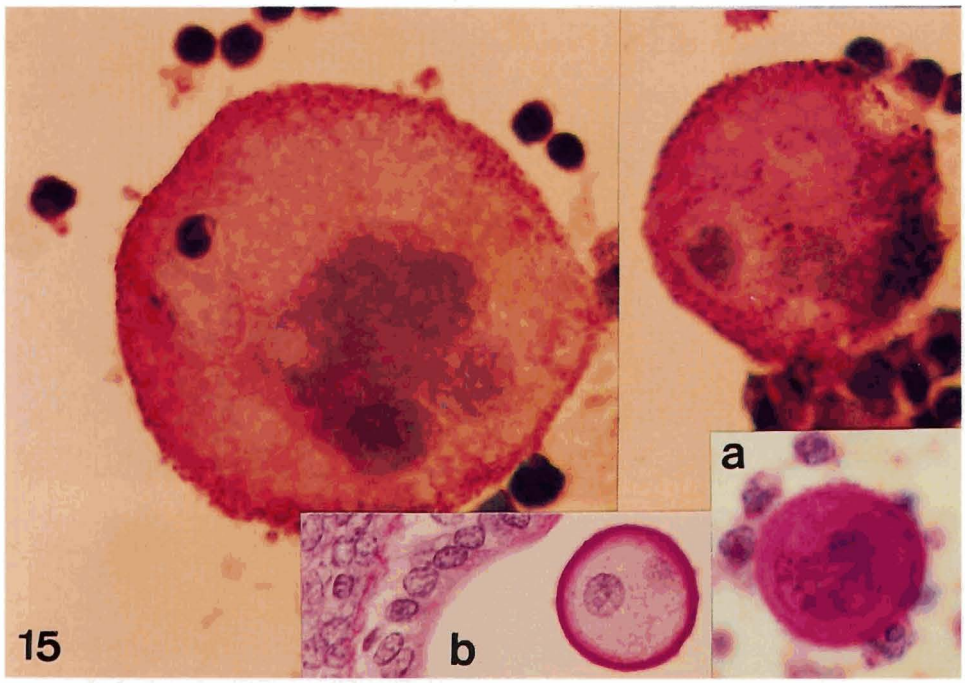

Fig. 15. Embryos in cultured AML cells show PAS-D positive DMs and minute chromosomes in the cortex. In situ PAS-D. x 1,000. **Inset a:** embryo in AML histological section showing a discrete cortex. PAS-D. x 1,000. **Inset b:** 2-cell rat embryo in uterus PAS-D. x 400

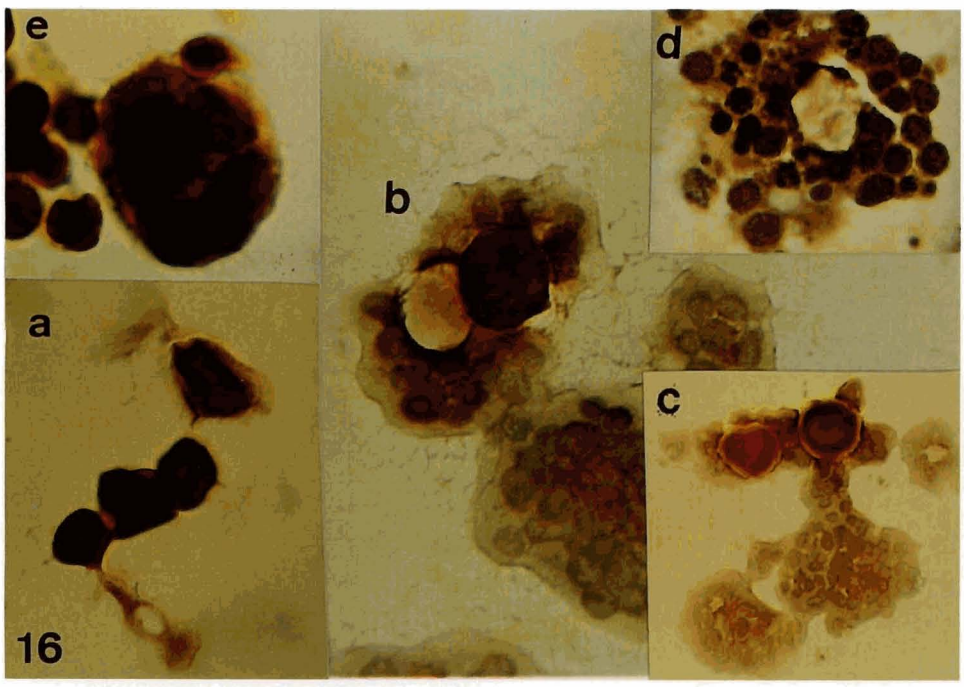

Fig. 16. α_1-antichymotrypsin in cultured AML cells. **Inset a:** conglomerated positive PGCs. α_1-antichymotrypsin. x 200. **Inset b:** positive PGC and NE of weak positive AGB. α_1-antichymotrypsin. x 400. **Inset c:** strong immunoreactivity in the content of AGB and NE. α_1-antichymotrypsin. x 200. **Inset d:** positive NV surrounding negative AGB in squash preparations. α_1-antichymotrypsin. x 400. **Inset e:** embryo with positive cells and NE. α_1-antichymotrypsin x 1,000

Fungal Og was fertilized by a fungal NV (Fig. 20b). The fungal Og formation was clear in PAS, PAS-D and immunostained squash preparations. Immunostained fungal cells or NCs extended nuclear segments around negative AGB, impregnated by positive NV and showed strongly positive conidiophores and conidiospores (ring chromosomes) (Fig. 20c). Fungal AGB, Og conidiospores and hyphae were PAS and PAS-D positive (Fig. 21). Fungal NCs (Fig. 21a) and globose 2-cell embryos (Fig. 21b) of positive PAS, PAS-D reaction resemble those of PGCs.

Rat testicular tissue squash preparations, also showed Og formation. Conglomerated PGC extended nuclear segments, forming the NE of Og (Fig. 22a-c). AGB impregnated by a spermatocytic NV was evident (Fig. 22a). Ogs of DMs and minute chromosomes were present (Fig. 22d). Ogs were abundant in clusters connected by nuclear segments in five-week-old rat testis (Fig. 22e). The general morphology of conglomerated PGC and Og in PAS-D-stained preparations resembled those in BMT (Fig. 22f). PGCs were present in all examined rat ages, dividing and migrating in two-week- (Fig. 23a), in the form of NV in five-week- (Fig. 23b) or with two large prominent nucleoli in eight-week-old rat testis (Fig. 23c). Invasion of testicular PGCs by a NV was observed (Fig. 23d). Testicular AGB also showed stained and unstained PAS-D areas (Fig. 23e). PAS positive AGB and Ogs were connected by nuclear segments in clusters (Fig. 23f), or encircled by crescentic epithelial cells (Fig. 23g), in five-week-old rat testis. Spermatocytic NVs fusing (invading or fertilizing) with another spermatocyte was demonstrated in five-week-old rat testis (Fig. 24a). Developing round embryos with a cortex, dissoluted nuclear material, NCs and nuclei or spermatocytes in meiosis observed in 4-week-old testis and smaller globose embryos in 1-week-old testis (Fig. 24c,d) document a common mechanism of cell renewal via embryo formation, in rapidly growing cells and tissues.

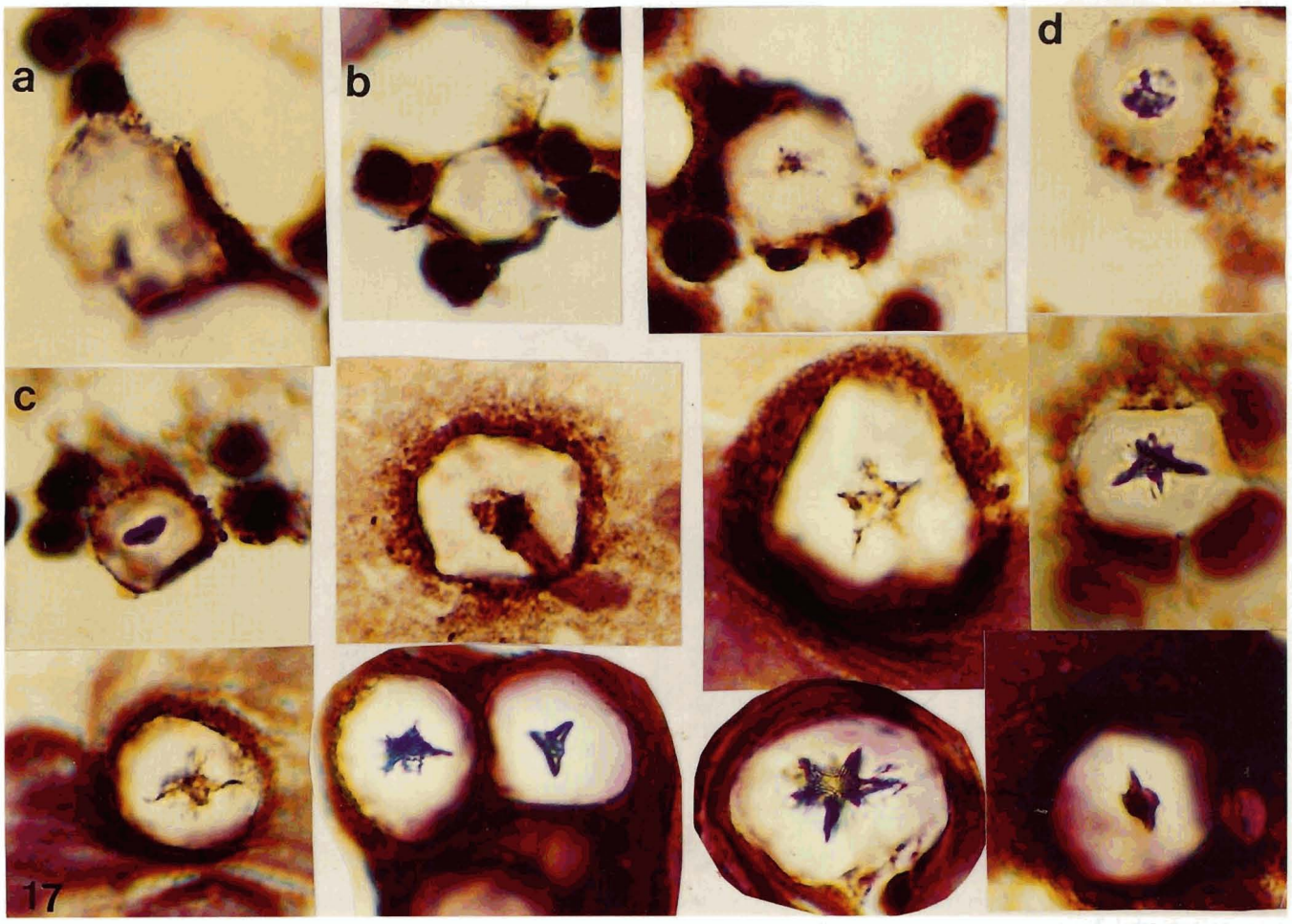

Fig. 17. Distribution of α_1-antichymotrypsin in squash preparations in AML. Weak positive or negative nuclear core of immature Ogs. **Inset a-c:** strongly immunostained nuclear segments embrace and form the NE of negative to weak positive AGBs. **Inset d:** mature Og with positive NE, negative plasma and nucleus. α_1-antichymotrypsin. x 1,000

Discussion

Before accepting the existence of PGCs, Ogs and embryos, it is necessary to rule out the possibility of artifactual observations. Firstly, talcum powder from rubber gloves and fungal contamination. Talcum powder slightly resembles immature Og and can contaminate samples during aspirate collection, but it cannot penetrate tissues in depth. Ogs identified in deep serial tissue section, being implanted and embraced by tissue cells or nuclear segments, excludes presence of talcum powder. Ogs due to fungal contamination are also excluded because all PAS-stained tissues were free of fungal cells and BMT aspirates tested on sabouraud agar gave no fungal growth. Secondly, it is necessary to rule out artifacts due to hypotonic treatment of tissue pieces. Hypotonic treatment breaks the extracellular matrix and cell membrane without affecting the integrity of nuclei and nuclear material. This is obvious in squash preparations where diffuse nuclear material co-exists with intact nuclei. Moreover, the repetitive observations shown in the three systems, squash preparations, cultured cells and tissue sections exclude the possibility of artifacts.

The main observation in this study is the existence of PGCs, Ogs, oocytes, fertilization and embryos in hematological malignancies in vivo, confirming previous in vitro study (Logothetou-Rella, 1996). It was evidenced that PGCs give rise to male (NVs) and female (oocytes) gametes. The female gamete originating from AGB developed through immature and mature Og, into a mature oocyte. NV, the male gamete, daughter cell of meiosis has been extensively discussed previously (Logothetou-Rella, 1994a,c, 1995a, 1996). Oocytes were fertilized by NV giving rise to embryo-like growth in the overall process of PGC-gametes-fertilization-embryo-

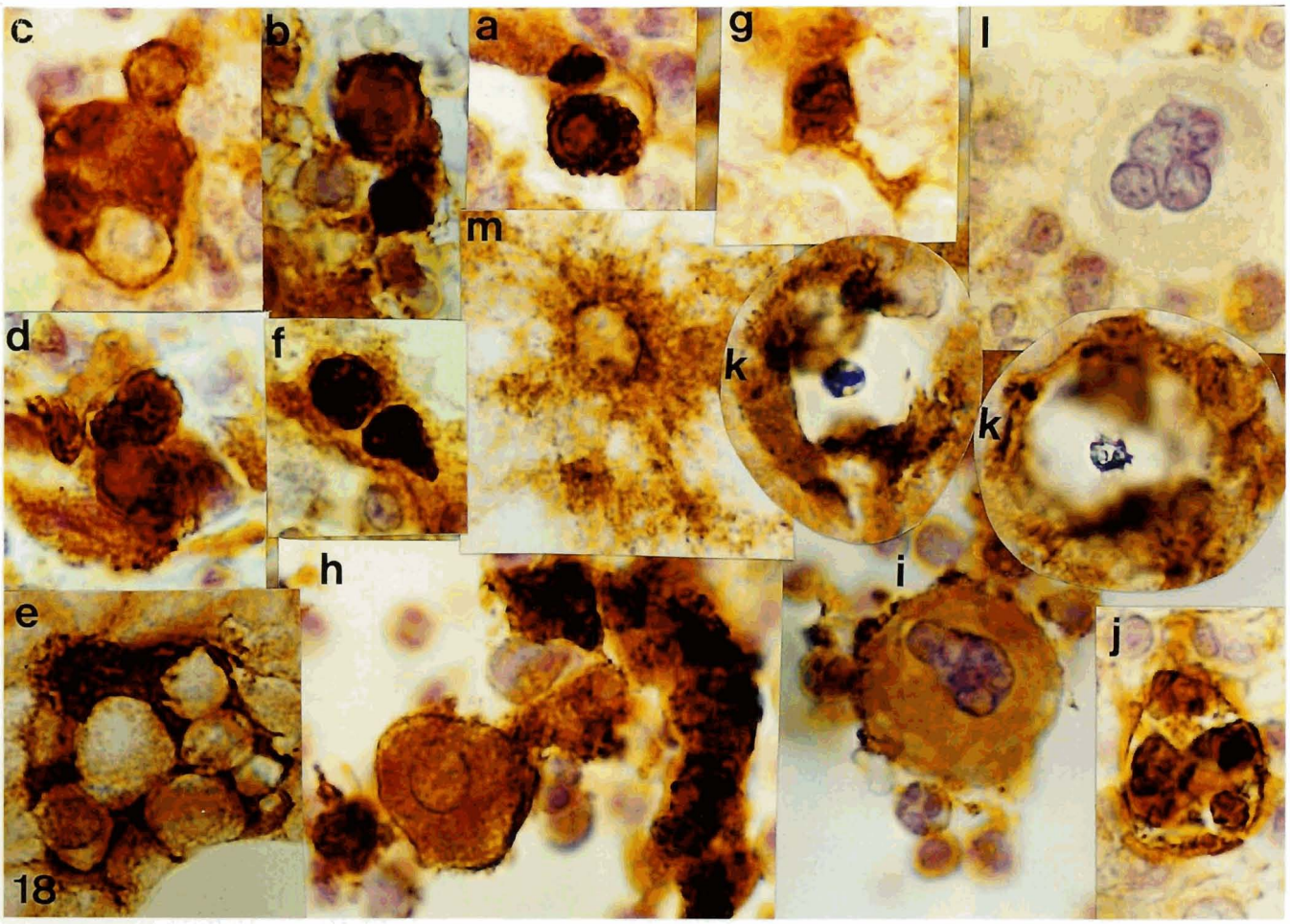

Fig. 18. Distribution of α_1-antichymotrypsin in AML tissue sections. **Inset a:** a positive PGC with prominent nucleoli giving rise to a positive NV. **Insets b-e:** conglomerated PGCs extend NV or nuclear segments embracing negative to positive AGBs. **Insets f and g:** PGCs in the shape of a NV with prominent nucleoli or conglomerated. **Inset h:** an oocyte-like cell with positive NE and plasma. Nearby NC is strongly positive. **Insets i and j:** small embryos with positive NE and/or cells. **inset k:** a mature Og with positive surrounding cells, NE, negative nucleus and plasma. **Inset l:** megakaryocyte is negative and shows no NE. **Inset m:** scattered immunoreactive chromosomes assemble around an AGB. α_1-antichymotrypsin. x 1,000

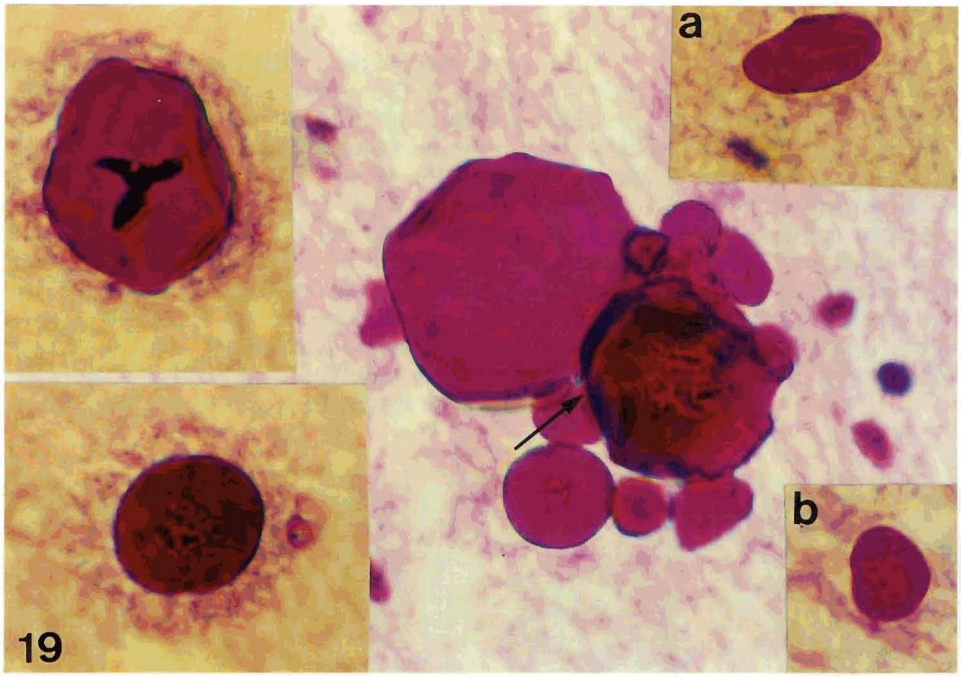

Fig. 19. GAG content in normal rat BMT. A PGC embraced by a NV (arrow) within a cluster of various-sized AGBs and immature Ogs. Single PGCs and immature Ogs are implanted in tissue matrix without adjacent cells. PAS. x 1,000. **Insets a and b:** PGCs. PAS-D. x 1,000

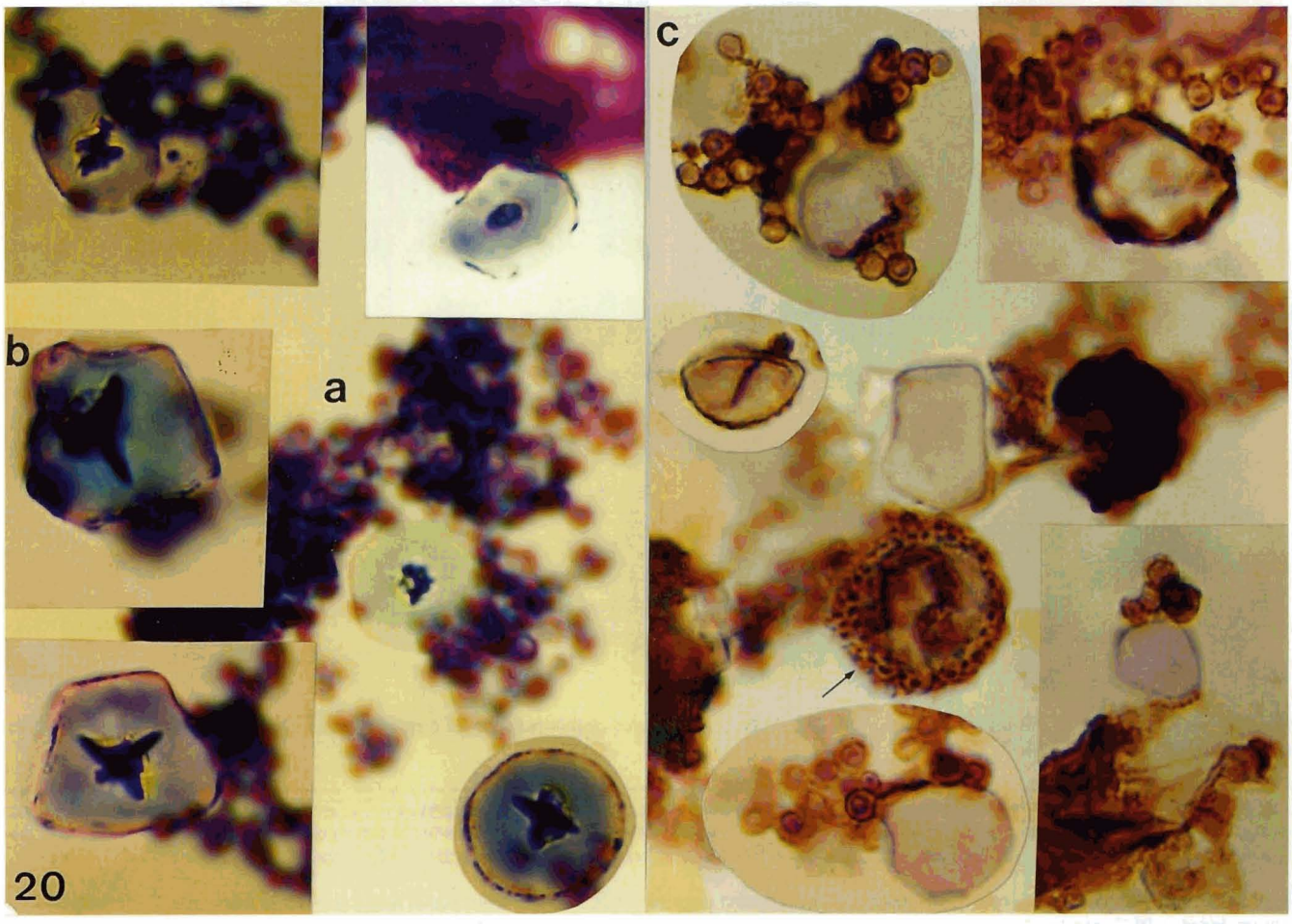

Fig. 20. Fungal cells. **Inset a:** Og with a round or star-shaped nuclear core and NE. **Inset b:** A NV fertilizing an Og. Giemsa. x 1,000. **Inset c:** positive cells or NC extend positive nuclear segments around negative AGB. Positive conidiophores and conidiospores (arrow). α_1-antichymotrypsin. x 1,000

PGC.

Very little information is available in the literature on PGCs, mainly from embryology. PGCs are first recognised in the yolk-sac endoderm, in early stages of embryonic development and eventually they migrate into the gonadal anlage where they differentiate and transform into spermatogonia (in male embryo) or oogonia (in female embryo) (Rabinovici and Jaffe, 1990). Because of this transformation, it was, until now, believed that PGCs disappeared upon fetal development of the gonads. Surprisingly enough, PGCs exist in normal BMT, malignant BMT and adult testis, as shown in this study.

It has been reported that PGCs can be recognized by their morphology, the positive PAS reaction of the cytoplasm and the high alkaline phosphatase activity in the cell membrane (Chiquoine, 1954; Falin, 1969; Rabinovici and Jaffe, 1990).

PGCs in BMT were evidenced by their large, migrating irregular, globose shape, the two prominent nucleoli, their encirclement by adjacent cells, single or syncytial and mainly by the intense PAS reaction (Falin, 1969; Kwang and Kennedy, 1973; Zamboni and Merchant, 1973; Fujimoto et al., 1977). These characteristics, when observed, clearly distinguish PGCs from all other cells in squash preparations, even at low

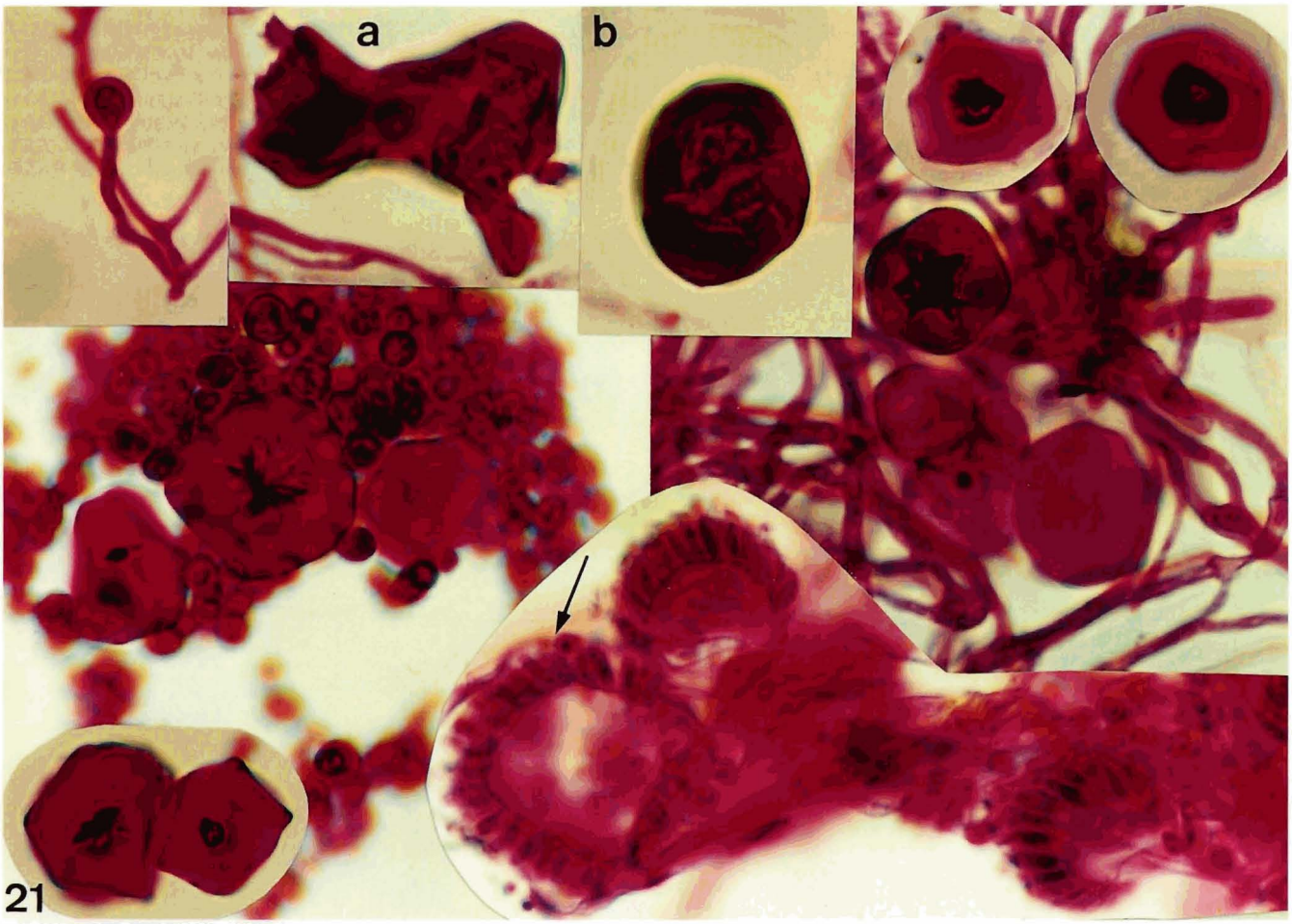

Fig. 21. GAG content of fungal cells. PAS-D positive Og, AGB, conidiophores and conidiospores (arrow). **Inset a:** fungal NC. **Inset b:** 2-cell fungal, globose embryo. PAS-D. x 1,000

Fig. 22. Testicular squash cell preparations from five- and six-week-old rats. **Insets a-c:** conglomerated (short arrow) PGC extends nuclear segments to Og. Spermatocytic NV has impregnated an AGB (long arrow). **Inset d:** immature Og with DMs and minute chromosomes. Giemsa. x 1,000. **Inset e:** Ogs in clusters connected with nuclear segments. Giemsa. x 200. **Inset f:** conglomerated PGC (arrows) with various Ogs in clusters. PAS-D. x 1,000

Fig. 23. Testicular squash cell preparations. **Insets a:** dividing and migrating PGCs in two-week-old rat. **Inset b:** PGC in the shape of NV in five-week-old rat. **Inset c:** PGC with two large prominent nucleoli in eight-week-old rat. **Inset d:** An NV invading a PGC. **Inset e:** AGB with stained and unstained areas embraced by nuclear segment. **Inset f:** Cluster of Ogs connected by nuclear segments. Figure focused on nuclear segments. PAS-D. x 1,000. **Inset g:** cluster of Ogs surrounded by crescentic cells. PAS-D. x 400

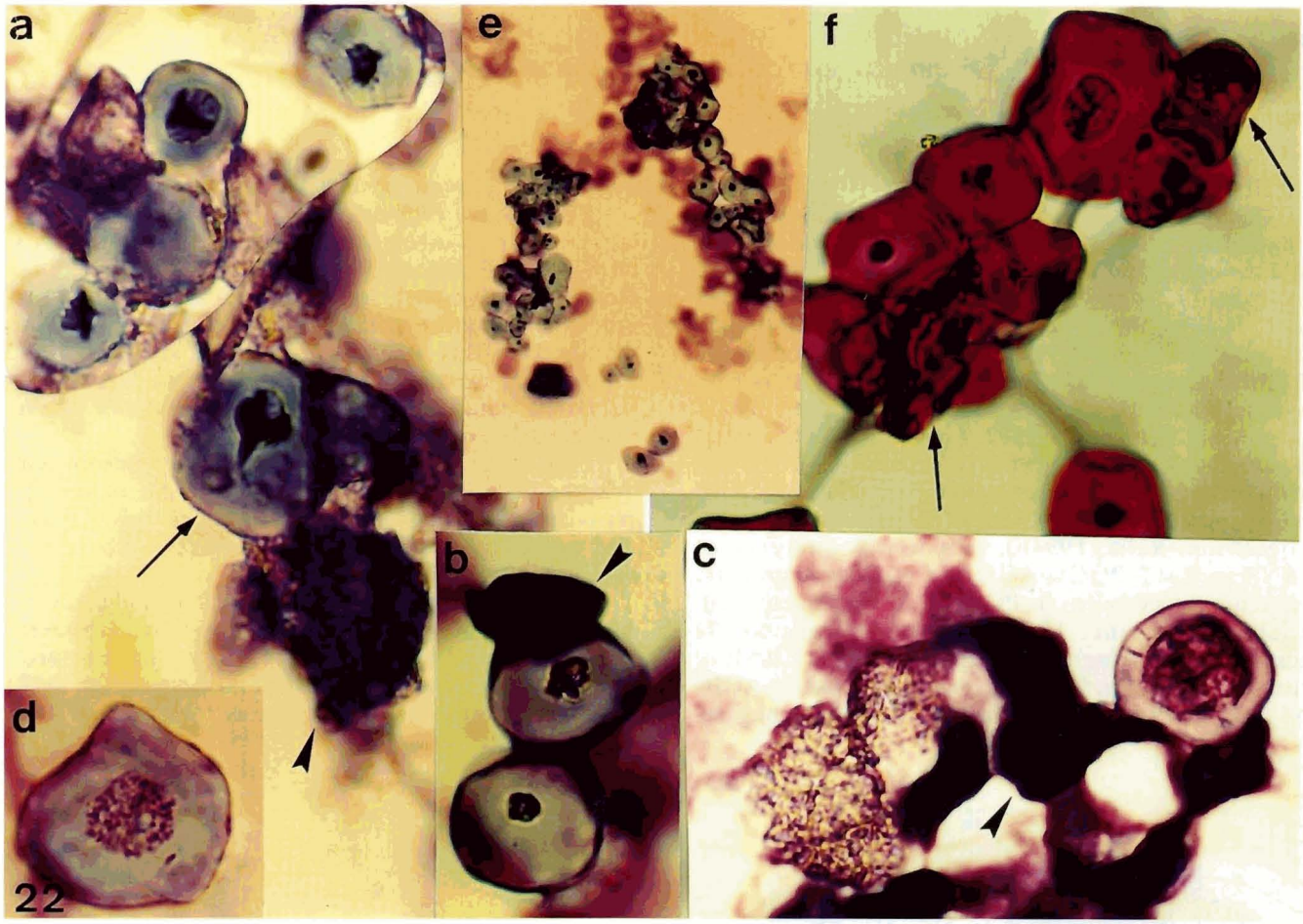
a
e
f
b
c
d
22

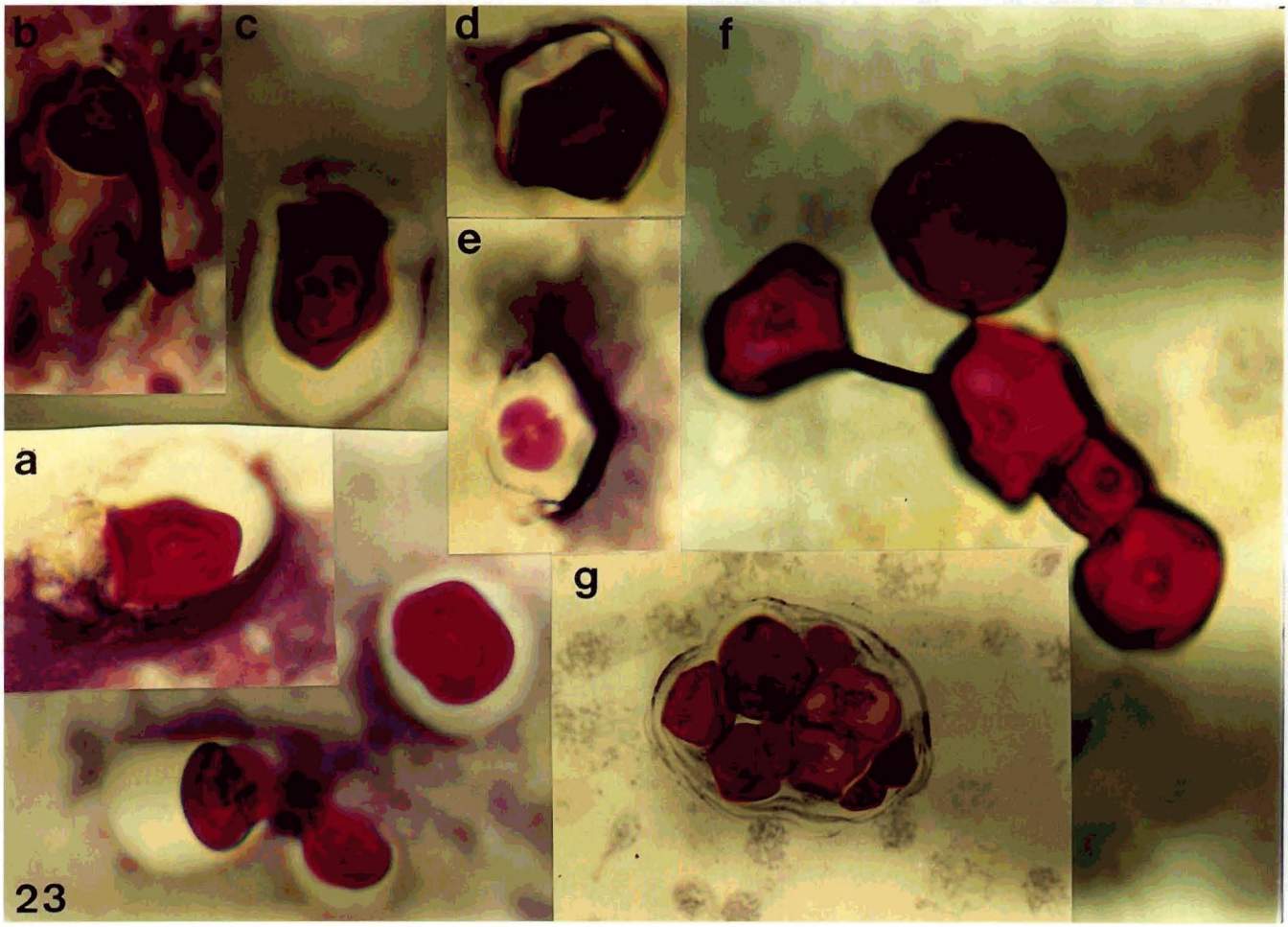
b
c
d
f
e
a
g
23

magnification.

The use of alkaline phosphatase as a marker for PGC (Chiquoine, 1954) has not been clear, because specific localization on PGCs has not been detected (Kwang and Kennedy, 1973) and it was therefore not used in this study. Instead, the antiserum against α_1-chymotrypsin was used to detect CANP activity due to unavailability of CANP antiserum and mainly because this antiserum cross-reacted with CANP in human meiotic malignant (Logothetou-Rella et al., 1992; Logothetou-Rella, 1996) and embryonic cells (Logothetou-Rella, 1995a). The fact that BMC have been sensitive to the inhibitor of CANP and insensitive to the inhibitor of trypsin-chymotrypsin (Logothetou-Rella, 1994b), supports the presence of CANP in BMT PGCs, AGB and nuclear segments. Existence of protease in PGCs is in agreement with others (Chiquoine, 1954; Fujimoto et al., 1977) regardless of it being alkaline phosphatase or CANP or other proteases. The high presence of protease in AGBs and absence in the cytoplasm of mature Ogs suggests involvement of protease in cell differentiation.

The positive PAS reaction of BMT and PGCs is in agreement with others reporting that embryonic PGCs contain high amounts of glycogen (Falin, 1969). However, glycogen has not been detected at the ultrastructural level (Zamboni and Merchant, 1973). For the first time, this study shows that PGCs contain GAG. Embryonic rat PGCs were also rich in GAG (unpublished data) documenting the resemblance of the fetal gonadal progenitors to those in BMT.

Fetal PGCs are the progenitors of spermatozoa and oocytes each developed in different male or female organisms. This study shows that PGCs give rise to NVs and oocytes within the same tissue which shows hermaphroditus behaviour.

It is not the purpose of the present investigation to survey in detail the field of spermatogenesis. However, testicular tissue was used in this study as a control system of high meiotic activity, possessing the self-renewal property. Testicular tissue is composed of stem

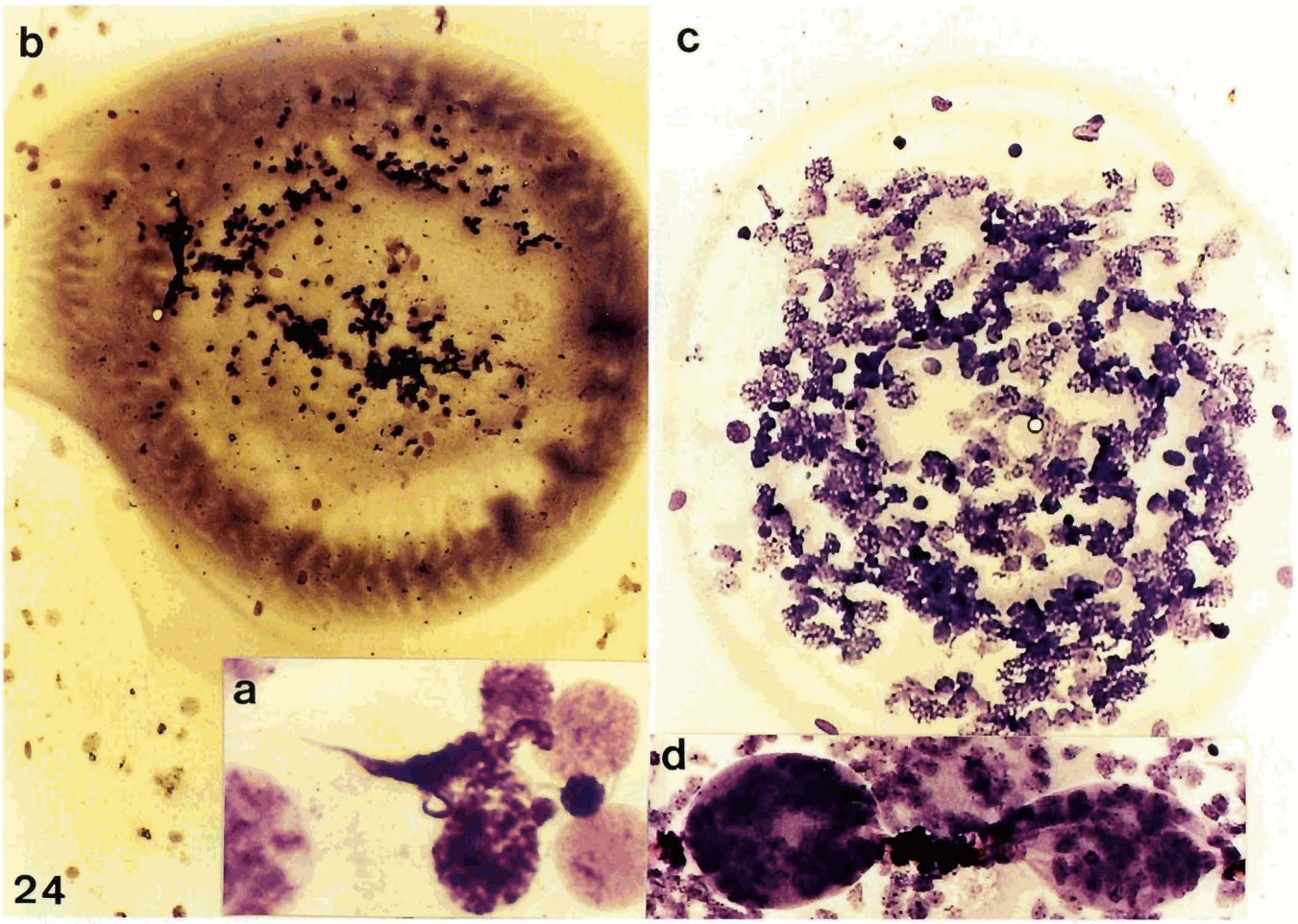

Fig. 24. Testicular squash cell preparations. **Inset a:** a spermatocytic NV fertilizing another spermatocyte. Giemsa. x 1,000. **Inset b:** early embryo with cortex of diffuse nuclear material and intact nuclei in the center, in four-week-old rat. Giemsa. x 100. **Inset c:** embryo with thin cortex and cells in meiosis, in four-week-old rats. Giemsa. x 200. **Inset d:** small globose embryos in one-week-old rat. Giemsa. x 200

cells (spermatogonia) and differentiating cells (spermatocytes, spermatozoa). The exact mode of stem cell renewal in testicular tissue, in many rapidly growing tissues, in embryos, in regeneration or in tumors has only recently been observed (unpublished data).

This study evidenced the existence of PGCs, NVs and embryo-like growth in adult rat testis, with a well correlated general morphology to those in BMT. This observation documents that the mode of stem cell renewal in rapidly growing tissues is identical, accomplished by the events: PGCs-gametes-fertilization-embryos. These events explain the arrangement in groups of «renewing testicular stem cells» and the «nodal» divisions (embryos) resulting in the equivalent in nature to production of new stem and differentiating cells (Clermont, 1972). The observations of this study are of direct relevance and strengthened by previous reports (Zamboni and Upadhya, 1983). It has been documented that PGCs in late fetal mouse adrenal glands always differentiated into oocytes, irrespective of the sex of the animal (Zamboni and Upadhya, 1983). However, these germ cells were characterized as ectopic mainly because the NV, the somatic male gamete, was unknown at the time and described only recently (Logothetou-Rella, 1994a, 1995a, 1996). Co-existence of oocytes, NVs and embryos in the same tissue in this study, suggests that germ cells observed in mouse adrenal glands were not ectopic gonadal PGC (Zamboni and Upadhya, 1983) but progenitors of adrenal gland cells, leading to development and growth of the fetal adrenal gland.

The present observations cannot be compared with previous studies on germ cells because the use of cytogenetic morphology is very recent (Logothetou-Rella, 1994a,c, 1995a, 1996) and the previous use of PAS reaction without hematoxylin counterstaining (Falin, 1969) does not allow follow up of PGC nuclear events. In order to avoid subjective interpretation, only the repetitive morphological observations are used to draw conclusions in this study. NVs and Og, are closely associated with nuclear conglomerates, NE is common to PGCs, AGBs, Og, and oocytes, arising from surrounding conglomerated cells or PGCs. NE consists of linear nuclear segment or DMs, and minute chromosomes. Surrounding conglomerated cells also produce NVs which impregnate AGBs, fertilize Ogs and oocytes, giving rise to various types of growing embryos. Embryos originated from fertilized PGCs (globose PGCs syncytia with NE), or Ogs and/or oocytes. Embryos show a cortex composed of glycoproteins, GAG and diffuse nuclear material. The cortex develops cells towards the embryo center. Hatching embryos result in extraembryonic release and dispersion of cells, which exhibit the growth characteristics described previously (Logothetou-Rella, 1996). Transformation of PGCs into oocytes and NVs involves gain or loss of GAG, glycoproteins, protease and nuclear material.

Due to the unavailability of normal human BMT (independent project in progress) direct comparison of this mechanism between normal and malignant tissues cannot be presented. However, the detection of PGCs, Ogs and NVs in normal rat BMT confirms the presence of identical mechanism in normal BMT. One obvious difference between malignant human and normal rat BMT was that in the latter, PGCs, AGBs and Ogs were not encircled by adjacent cells and the few embryos present were devoid (hollow) of cells.

The present observations support the clonal evolution of malignant cell populations (McCulloch, 1983) and provide further information on the morphology and behaviour of stem cells. PGCs are the primary stem cells giving rise to secondary germ cells, the oocytes and NVs. Cells in embryos are indeed the descendants of a single progenitor, the PGC. The origin of neoplasia may lie in the primary stem cells or in the secondary germ cells (McCulloch, 1983). PGCs and germ cells are the cell renewal source of a neoplasm capable of serving as the seeds of metastatic spread of cancer due to their migrating property and CANP content.

The identification of PGCs in two different organs (testis and BMT) from different mammals (human-rat) documents that PGCs are tissue specific.

NV formation by meiosis and fertilization has already been reported on rapidly growing embryonic cells (Logothetou-Rella, 1995a), virally-infected cells (Logothetou-Rella, 1995b), PHA-activated lymphocytes (Logothetou-Rella, 1994c), malignant cells from solid (Logothetou-Rella, 1994a) and hematological tumors (Logothetou-Rella, 1996). The present observations reveal additional information on PGCs, Ogs and embryos.

The morphology of fungal germ cells, NCs and embryos, closely resembling that of BMT and testicular tissues, can lead to negligence of and mislead the present observations. Tissue sectioning, at less than 5 μm thickness, displaces germ cells and embryos due to their globose shape; displaced germ cells can then be evaluated as fungal contamination or artifacts and be neglected. Moreover, the high morphological and enzymatic resemblance of fungal with mammalian tissue germ cells and embryos, strongly documents identical life cycle involving meiosis.

The cytogenetic morphology of fungal Ogs, arisen from AGBs within NCs, is identical in BMT, testicular and other tissues (unpublished data), involving GAG, glycoproteins, protease and nuclear material. It is therefore evident that Ogs are fabricated de novo from the interaction of GAG and NV and do not pre-exist. The present observations raise many questions and support the general hypothesis that residual, discarded bodies of differentiating cells, fused into NCs, provide the material for the novo fabrication of PGCs. NCs, previously considered to be inert products of cell degeneration, are nuclear pools formed by discarded meiotic cells (Logothetou-Rella, 1995a, 1996) and mainly composed of blended nuclear material with

GAG, glycoproteins and CANP. The fact that NCs of PGCs give rise to Ogs and NVs, documents that NCs are functional.

More work is in progress for further information on the stem cell renewal mechanism.

Acknowledgements. The author is indebted to Mrs. M. Skoura and Mrs. E. Katsarou for their expert technical assistance and Mr. C.E. Harissis for his kind provision of a Nikon phase contrast microscope. The author wishes to thank Professor C. Kittas and S. Patsouris for providing bone marrow paraffin-embedded tissues, and the General Secretary of Research and Technology for supporting this project with the grant No 288.

References

Chiquoine D.A. (1954). The identification, origin and migration of the primordial germ cells in the mouse embryo. Anat. Rec. 118, 135-145.

Clermont Y. (1972). Kinetics of spermatogenesis in mammals: seminiferous epithelium cycle and spermatogonial renewal. Physiol. Rev. 52, 198-236.

Falin L.I. (1969). The development of genital glands and the origin of germ cells in human embryogenesis. Acta Anat. 72, 195-232.

Fujimoto T., Miyayama Y. and Fuyuta M. (1977). The origin, migration and fine morphology of human primordial germ cells. Anat. Rec. 188, 315-330.

Hsu S.M., Raine L. and Fanger H. (1981). A comparative study of the peroxidase-antiperoxidase method and an avidin-biotin complex method for studying polypeptide hormones with radioiummunoassay antibodies. Am. J. Clin. Pathol. 75, 734-738.

Kwang W.J. and Kennedy J.R. (1973). The primordial germ cells in early mouse embryos: light and electron microscopic studies. Dev. Biol. 31, 275-284.

Logothetou-Rella H., Karayannis A., Vamvassakis E., Livaditou A., Pikramenos D., Nesland J.M. and Dimopoulos C. (1992). A cytologic, ultrastructural and immunocytochemical comparison of tumor cells and cell cultures originating in invasive bladder carcinoma. Eur. Urol. 21, 146-150.

Logothetou-Rella H. (1994a). Cytogenetic analysis and morphology of malignant nuclear vlimata. The life cycle of malignant cells. Histol. Histopathol. 9, 747-763.

Logothetou-Rella H. (1994b). The selective anticancer activity of the endogenous inhibitor of calcium-activated neutral proteinase. A histological, cytological and chemosensitivity study. Histol. Histopathol. 9, 485-493.

Logothetou-Rella H. (1994c). Differentiation of human lymphocytes into nuclear vlimata by meiosis. The cytotoxic effect of calcium-activated neutral proteinase inhibitor. Histol. Histopathol. 9, 469-484.

Logothetou-Rella H. (1995a). Nuclear vlimata and aneuploidy in embryonic cells is caused by meiosis. Behavior and properties of meiotic cells. Histol. Histopathol. 10, 541-566.

Logothetou-Rella H. (1995b). The inhibitor of calcium-activated neutral proteinase is an anti-meiotic agent. The spermicidal and anti-viral action. Histol. Histopathol. 10, 271-282.

Logothetou-Rella H. (1996). Meiosis in hematologic malignancies. In situ cytogenetic morphology. Histol. Histopathol. 11, 943-963.

McCulloch E.A. (1983). Stem cells in normal and leukemic hemopoiesis. Blood 62, 1-13.

Plachot M., de Grouchy J., Junca A.M., Mandelbaum J., Turleau C., Coullin P., Cohen J. and Salat-Baroux J. (1987). From oocyte to embryo: A model, deduced from in vitro fertilization, for natural seclection against chromosome abnormalities. Ann. Genet. 30, 22-32.

Rabinovici J. and Jaffe R.B. (1990). Development and regulation of growth and differentiated function in human and subhuman primate fetal gonads. Endocr. Rev. 11, 532-557.

Zamboni L. and Merchant H. (1973). The fine morphology of mouse primordial germ cells in extragonadal locations. Am. J. Anat. 137, 236-299.

Zamboni L. and Upadhya Y. (1983). Germ cell differentation in mouse adrenal glands. J. Exp. Zool. 228, 173-183.

Accepted June 10, 1996